

Discovery of GluN2A-Selective NMDA Receptor Positive Allosteric Modulators (PAMs): Tuning Deactivation Kinetics via Structure-Based Design

Matthew Volgraf,^{*,†} Benjamin D. Sellers,[†] Yu Jiang,[▽] Guosheng Wu,[▽] Cuong Q. Ly,[†] Elisia Villemure,[†] Richard M. Pastor,[†] Po-wai Yuen,[▽] Aijun Lu,[▽] Xifeng Luo,[▽] Mingcui Liu,[▽] Shun Zhang,[▽] Liang Sun,[▽] Yuhong Fu,[▽] Patrick J. Lupardus,^{||} Heidi J.A. Wallweber,^{||} Bianca M. Liederer,[⊥] Gauri Deshmukh,[⊥] Emile Plise,[⊥] Suzanne Tay,[⊥] Paul Reynen,[§] James Herrington,[§] Amy Gustafson,[§] Yichin Liu,[§] Akim Dirksen,[¶] Matthias G. A. Dietz,[¶] Yanzhou Liu,[‡] Tzu-Ming Wang,[‡] Jesse E. Hanson,[‡] David Hackos,[‡] Kimberly Searce-Levie,[‡] and Jacob B. Schwarz[†]

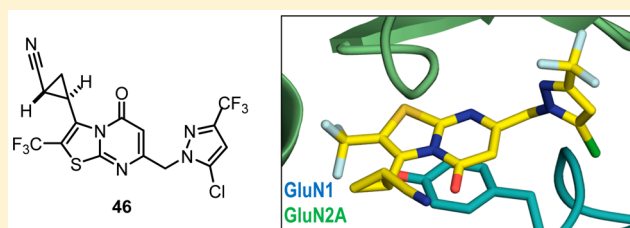
[†]Department of Discovery Chemistry, [‡]Department of Neurosciences, [§]Department of Biochemical and Cellular Pharmacology, [⊥]Department of Drug Metabolism and Pharmacokinetics, and ^{||}Department of Structural Biology, Genentech, Inc., 1 DNA Way, South San Francisco, California 94080, United States

[▽]Pharmaron-Beijing Co. Ltd., 6 Taihe Road, BDA, Beijing 100176, PR China

[¶]Ion Channels Group, Evotec AG; Manfred Eigen Campus, Essener Bogen 7, 22419 Hamburg, Germany

S Supporting Information

ABSTRACT: The *N*-methyl-D-aspartate receptor (NMDAR) is a Na⁺ and Ca²⁺ permeable ionotropic glutamate receptor that is activated by the coagonists glycine and glutamate. NMDARs are critical to synaptic signaling and plasticity, and their dysfunction has been implicated in a number of neurological disorders, including schizophrenia, depression, and Alzheimer's disease. Herein we describe the discovery of potent GluN2A-selective NMDAR positive allosteric modulators (PAMs) starting from a high-throughput screening hit. Using structure-based design, we sought to increase potency at the GluN2A subtype, while improving selectivity against related α -amino-3-hydroxy-5-methyl-4-isoxazolepropionic acid receptors (AMPA). The structure–activity relationship of channel deactivation kinetics was studied using a combination of electrophysiology and protein crystallography. Effective incorporation of these strategies resulted in the discovery of GNE-0723 (**46**), a highly potent and brain penetrant GluN2A-selective NMDAR PAM suitable for *in vivo* characterization.



■ INTRODUCTION

Glutamate is the primary excitatory neurotransmitter in the mammalian brain and acts on several membrane-bound receptors, including both metabotropic receptors (mGluRs) and ionotropic receptors (iGluRs).¹ iGluRs are subdivided according to their function and pharmacology including α -amino-3-hydroxy-5-methyl-4-isoxazolepropionic acid receptors (AMPA), kainate receptors, and *N*-methyl-D-aspartate receptors (NMDARs). NMDARs are tetrameric assemblies including two GluN1 and two GluN2 subunits that bind the coagonists glycine and glutamate, respectively. The four GluN2 subtypes (GluN2A, GluN2B, GluN2C, and GluN2D) largely determine the receptor's functional and spatiotemporal expression heterogeneity. Functionally, NMDARs are blocked by Mg²⁺ at resting membrane potential and require both agonist binding and cell depolarization to open the trans-membrane channel. Within the nervous system, NMDARs are implicated in controlling synaptic plasticity and are therefore

thought to underlie both memory formation and other higher cognitive functions.²

Due to their central role in neurotransmission, NMDARs have attracted significant interest as pharmacological targets. Memantine, a nonselective NMDAR antagonist, has been approved for treatment of moderate-to-severe Alzheimer's disease,³ while GluN2B-selective antagonists such as ifenprodil, have been studied as neuroprotective agents.⁴ NMDAR hypofunction has long been implicated in the pathophysiology of schizophrenia beginning with the discovery that the dissociative anesthetics ketamine and phencyclidine (PCP) induce a psychotomimetic state resembling the disease while functioning as noncompetitive NMDAR antagonists.⁵ More recently, NMDARs have been shown to regulate γ oscillations generated by fast-spiking (FS) parvalbumin (PV) interneurons, a cellular subtype that controls the inhibition of excitatory

Received: December 26, 2015

Published: February 26, 2016

neurons.⁶ EEG studies have further demonstrated that γ oscillations are disrupted in schizophrenic patients, strengthening the link between NMDAR dysfunction and schizophrenia.⁷

Recently, a number of NMDAR positive allosteric modulators (PAMs) have been reported in the literature targeting NMDAR hypofunction. Endogenous nonselective NMDAR PAMs have been found, including the neurosteroid pregnenolone sulfate,⁸ along with the brain cholesterol metabolite 24(S)-hydroxycholesterol and closely related analogs.⁹ Subunit selective PAMs have also been described,^{10–12} including the GluN2C/2D selective CIQ.

Our goal was to enhance physiological NMDAR activation while avoiding potentially toxic overactivation. Therefore, we focused on discovering PAMs that are selective for NMDARs containing the GluN2A subunit, which is broadly distributed in the mature brain and located at synapses.¹³ At the same time, selectivity against NMDARs containing only GluN2B subunits avoids the potential toxic consequences of overstimulating extrasynaptic GluN2B-containing NMDARs.^{14,15} We believed the identification of GluN2A selective NMDAR PAMs would help dissect the physiological role of NMDAR subtypes in disease and neuronal function while also providing a novel therapeutic approach in schizophrenia and other neurological disorders.¹⁶

Here we report the discovery and optimization of a series of GluN2A-selective PAMs starting from the high throughput screening hit **1** (Table 1), which displayed low micromolar

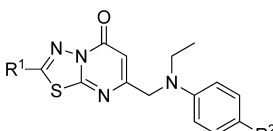
meric receptors as well as pyramidal neuron and interneuron NMDAR responses.¹⁷

The GluN2A potency of **1** was quickly optimized by truncating the butyl chain to a methyl (compound **2**) and adding a fluorine at the 4-position of the aniline (compound **3**), while maintaining selectivity against GluN2B. Compound **3** provided an excellent starting point for a focused lead optimization campaign despite the poor observed selectivity against AMPARs (GluA2_{flip} and GluA2_{flipop} isoforms). Electrophysiology revealed that **3** and related PAMs slowed channel deactivation kinetics as the primary means of potentiation, a characteristic we sought to minimize in order to preserve the timing and rhythm of neural firing patterns.¹⁷ The CNS drug-like properties of **3** were also favorable; the measured log *D* was moderate (<3), topographical polar surface area (TPSA) was low (<90 Å²), and there was no observable P-glycoprotein (P-gp) efflux *in vitro* (efflux ratio < 3).¹⁸ However, poor metabolic stability, both in liver microsomes and *in vivo* (data not shown), prevented the use of **3** as an *in vivo* tool compound. Because metabolite identification studies revealed N-dealkylation as the major metabolic pathway for this series of PAMs (data not shown), efforts to replace the *N*-ethyl aniline and increase overall potency while maintaining CNS drug-like properties became a top priority.

RESULTS AND DISCUSSION

A cocrystal structure of **2** was obtained, using truncated GluN2A and GluN1 ligand-binding domains (LBDs) (Figure 1A).¹⁹ The structure revealed a binding site at the dimer interface of the GluN1–GluN2A LBD,¹⁷ the same site observed in the closely related AMPARs, where PAM binding stabilizes the LBDs in their closed-cleft, ligand-bound conformations.²⁰ It was therefore unsurprising that **1** and

Table 1. HTS Hit **1** and Optimized Tool Compounds **2** and **3**



Compound 3:
MW: 318 g/mol
LogD: 2.9
TPSA: 50 Å²
LM^b H/R/M^c (mL/min/kg): 5 / 48 / 82
MDR1^d P-gp ER^e (B:A/A:B): 1.4

EC ₅₀ (max potentiation), ^a μM (%)						
ex	R ¹	R ²	GluN2A	GluN2B	GluA2 _{Flip}	GluA2 _{Flop}
1	<i>n</i> -Bu	H	9.34 (91)	(40)	35.2 (51)	23.7 (71)
2	Me	H	1.9 (150)	(35)	7.5 (84)	2.0 (95)
3	Me	F	0.90(150)	(48)	3.3 (92)	0.83 (99)

^aNMDAR EC₅₀ values were determined in the presence of EC₃₀ glutamate and saturating glycine. Max potentiation (%) at 125 μM is reported if no EC₅₀ could be obtained, where 30% denotes the assay baseline (EC₃₀ glutamate). AMPAR EC₅₀ values were determined in the presence of 100 μM glutamate using the AMPA receptor PAM LY450108 as a positive control at 100%. Max potentiation (%) at 125 μM is reported if no EC₅₀ could be obtained, where 0% denotes the assay baseline due to receptor desensitization. All EC₅₀ values represent geometric means of at least two determinations. ^bLiver microsome-predicted hepatic clearance. ^cH/R/M = human/rat/mouse. ^dMDCK-MDR1 human P-gp transfected cell line. ^eEfflux Ratio. ^fBasolateral-to-apical/apical-to-basolateral.

potency against GluN2A and minimal activity against GluN2B. Compound **1** and related molecules from this series have been previously confirmed to act as allosteric modulators rather than orthosteric ligands via electrophysiology, where compound alone resulted in little to no observable current, while significant potentiation was observed in the presence of glutamate.¹⁷ Additional pharmacological studies have also been reported, including effects on GluN2A/GluN2B trihetero-

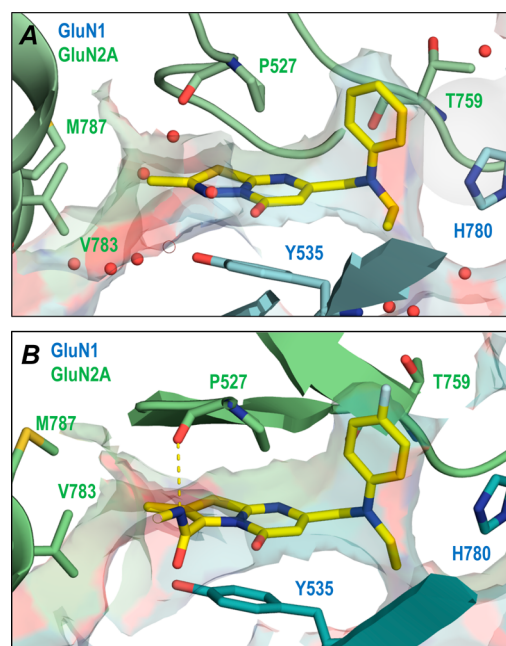
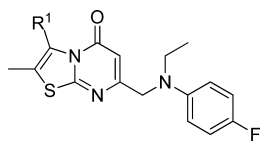
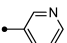
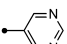
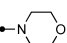
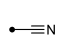
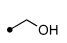
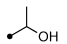
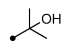
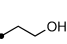
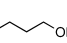
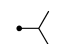
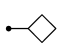

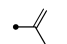
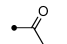
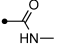
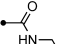


Figure 1. Crystal structure of **2** (A) and **19** (B) bound to the GluN1/GluN2A ligand binding domain (PDB codes: 5H8H and 5I2K, respectively). Solvent accessible surface rendering depicts the binding site with relevant amino acids denoted by their single amino acid code. Blue coloring represents residues from GluN1 and green coloring represents residues from GluN2A.

Table 2. Representative Examples of C'-Subsite SAR



Ex	R ¹	EC ₅₀ (Max potentiation) ^a μM (%)			LM ^b H/R/M ^c (mL/min/kg)	MDR1 ^d P-gp ER ^e (B:A:A:B) ^f
		GluN2A	GluA2 _{Flip}	GluA2 _{Flop}		
4	•H	0.312 (150)	0.252 (95)	0.245 (93)	15 / 50 / 82	1.0
5	• 	0.168 (144)	33.8 (75)	4.5 (11)	19 / 48 / 84	1.2
6	• 	0.137 (148)	(56)	0.972 (16)	18 / 46 / 83	1.2
7	• 	2.2 (69)	75.8 (11)	60.2 (8)	18 / 49 / 83	0.9
8	• 	0.129 (181)	66.6 (13)	10.7 (60)	14 / 50 / 83	0.9
9	• 	0.649 (153)	66.3 (39)	1.9 (83)	12 / 49 / 83	1.1
10 ^g	• 	0.183 (154)	32.3 (37)	5.5 (30)	16 / 48 / 82	0.6
11	• 	0.063 (157)	12.4 (65)	2.4 (5)	17 / 49 / 83	1.0
12	• 	0.159 (168)	10.5 (72)	0.572 (75)	13 / 48 / 82	0.9
13	• 	0.183 (169)	33.2 (37)	1.5 (45)	15 / 46 / 82	1.0
14	• 	0.685 (129)	34.4 (15)	(1)	18 / 47 / 79	1.3
15	• 	2.6 (122)	35.9 (38)	8.6 (20)	ND ^h	ND
16	• 	0.394 (168)	34.0 (35)	9.8 (31)	18 / 46 / 82	0.8
17	• 	0.060 (143)	43.1 (75)	13.0 (22)	ND	ND
18	• 	0.088 (173)	(13)	9.4 (55)	15 / 48 / 80	1.1
19	• 	0.131 (185)	(18)	(38)	5 / 46 / 84	9.8
20	• 	0.093 (184)	(10)	(28)	10 / 46 / 82	5.1

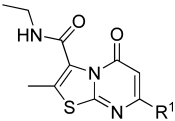
^aNMDAR EC₅₀ values were determined in the presence of EC₃₀ glutamate and saturating glycine. Max potentiation (%) at 125 μM is reported if no EC₅₀ could be obtained, where 30% denotes the assay baseline (EC₃₀ glutamate). AMPAR EC₅₀ values were determined in the presence of 100 μM glutamate using the AMPA receptor PAM LY450108 as a positive control at 100%. Max potentiation (%) at 125 μM is reported if no EC₅₀ could be obtained, where 0% denotes the assay baseline due to receptor desensitization. All EC₅₀ values represent geometric means of at least two determinations. ^bLiver microsome-predicted hepatic clearance. ^cH/R/M = human/rat/mouse. ^dMDCK-MDR1 human P-gp transfected cell line. ^eEfflux ratio. ^fBasolateral-to-apical/apical-to-basolateral. ^gRacemate. ^hND = not determined.

related analogs significantly potentiated AMPARs in addition to GluN2A-containing NMDARs. We hypothesized that the selectivity of this class of PAMs against other GluN2 subunits could be attributed to van der Waals interactions with Val783 of GluN2A at the dimer interface. In the other subtypes, this residue is a phenylalanine (GluN2B) or leucine (GluN2C and GluN2D), while the GluA2 flip and flop isoforms possess the polar residues serine and asparagine, respectively. After

recognizing that selectivity against GluA2 receptors would be a concern for this series of PAMs, GluA2_{flip} and GluA2_{flop} calcium imaging assays were established as the major counter-screen assay, while GluN2B/C/D selectivity panels were obtained much less frequently.

The crystal structure revealed a clear opportunity for increasing receptor interactions by building into a water-filled pocket proximal to the thiadiazole-core nitrogen, in a region we

Table 3. Representative Examples of Aromatic SAR at the Core Benzylic Position



Ex	R ¹	EC ₅₀ (Max potentiation) ^a			LM ^b H/R/M ^c (mL/min/kg)	MDR1 ^d P-gp ER ^e (B:A:A:B) ^f
		GluN2A	μ M (%) GluA2 _{Filip}	GluA2 _{Flop}		
21		0.132 (171)	(5)	48.7 (32)	12 / 46 / 83	12.6
22		0.434 (159)	(2)	(2)	7 / 27 / 75	8.6
23		7.0 (123)	(8)	(19)	7 / 11 / 58	5.8
24		1.7 (170)	(6)	(13)	6 / 31 / 74	22
25		8.5 (77)	(11)	(15)	2 / 3 / 26	2.0
26		62.2 (71)	32.9 (10)	53.7 (8)	2 / 10 / 25	25
27		1.9 (113)	(18)	66.2 (21)	3 / 3 / 61	20
28		9.1 (102)	(3)	(3)	4 / 7 / 30	3.1
29		1.2 (94)	28.3 (9)	29.4 (20)	5 / 11 / 50	1.8
30		12.9 (94)	(1)	(0)	2 / 10 / 46	22
31		17.5 (102)	(2)	(2)	5 / 11 / 56	44
32 ^g		3.1 (75)	(4)	(8)	3 / 12 / 60	2.2
33		17.0 (99)	(2)	(1)	5 / 8 / 12	21.5
34		4.9 (128)	(8)	(19)	2 / 0.5 / 11	33
35		0.436 (120)	37.0 (8)	73.2 (16)	3 / 9 / 40	11
36		0.536 (147)	(54)	6.4 (60)	4 / 16 / 58	2.2
37		0.414 (144)	(32)	9.1 (43)	3 / 12 / 81	57
38		57.1 (60)	(3)	(10)	9 / 38 / 82	3.7

^aNMDAR EC₅₀ values were determined in the presence of EC₃₀ glutamate and saturating glycine. Max potentiation (%) at 125 μ M is reported if no EC₅₀ could be obtained, where 30% denotes the assay baseline (EC₃₀ glutamate). AMPAR EC₅₀ values were determined in the presence of 100 μ M glutamate using the AMPA receptor PAM LY450108 as a positive control at 100%. Max potentiation (%) at 125 μ M is reported if no EC₅₀ could be obtained, where 0% denotes the assay baseline due to receptor desensitization. All EC₅₀ values represent geometric means of at least two determinations. ^bLiver microsome-predicted hepatic clearance. ^cH/R/M = human/rat/mouse. ^dMDCK-MDR1 human P-gp transfected cell line. ^eEfflux ratio. ^fBasolateral-to-apical/apical-to-basolateral. ^gRacemate.

termed the C'-subsite based on similarity to the AMPAR PAM pocket.²¹ We hypothesized that by displacing these crystallographic waters we might gain significant GluN2A potency. To achieve this, we replaced the thiadiazole-based core of **1** with a thiazole-based scaffold and sought to explore substitution at the newly created carbon center with a variety of functional groups.

We believed that substitution at this position might yield more selective PAMs against AMPARs, because comparison of the binding sites from the two receptors suggested that the C'-subsite of GluN2A was larger than the corresponding pocket in GluA2. Therefore, we hypothesized that larger groups at this position might afford both additional potency and selectivity.

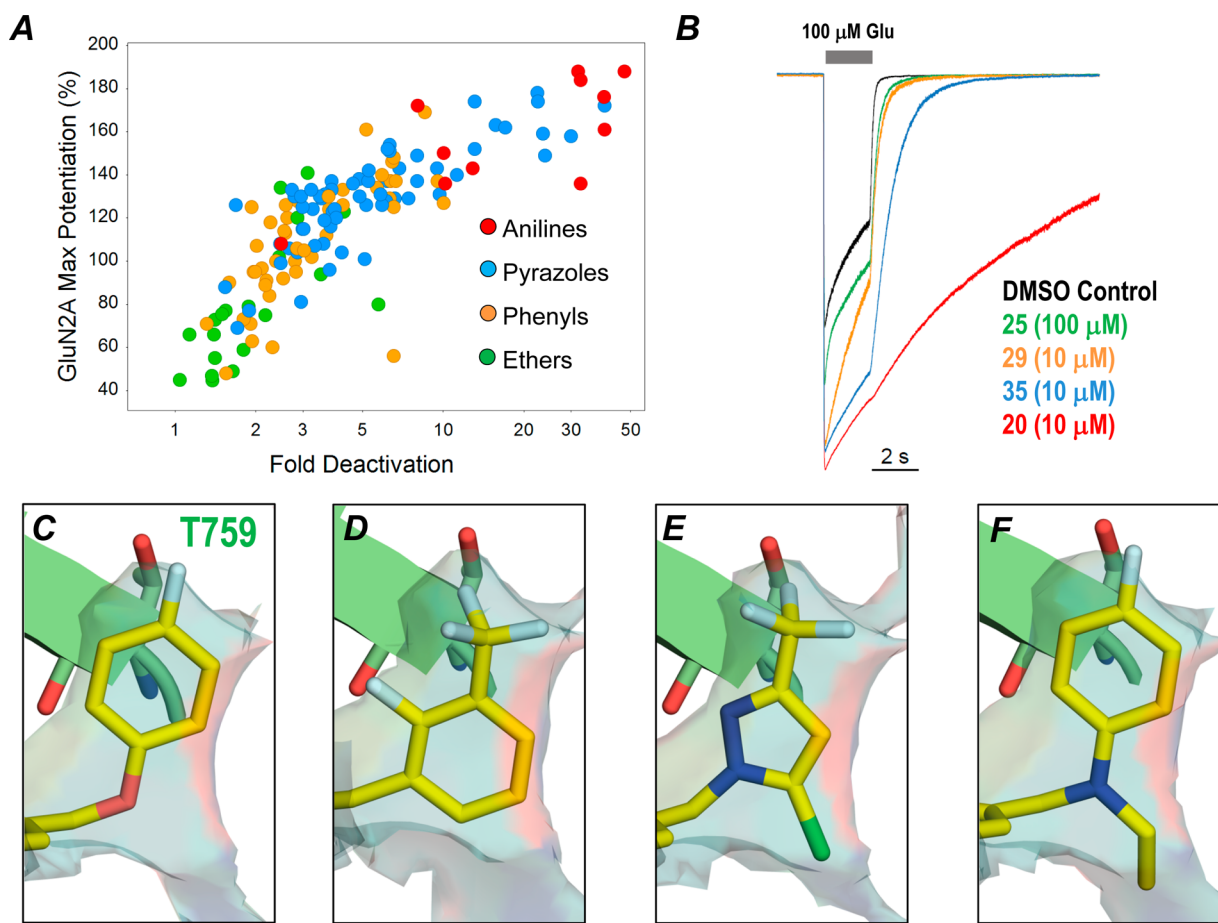


Figure 2. (A) Relationship between GluN2A max potentiation (%) and fold deactivation as measured via automated electrophysiology experiments in CHO cells. Colors denote identity of functional group at the benzylic position of the core. (B) Overlay of whole cell voltage clamp recordings comparing PAM properties and deactivation kinetics for matched pairs **20**, **25**, **29**, and **35**. (C–F) Representative crystal structure detail of aromatic groups at the benzylic position of the thiadiazolopyrimidine core. Compounds depicted are **40** (C), **29** (D), **46** (E), and **19** (F) (PDB codes 5H8R, 5I2N, 5I2J, and 5I2K, respectively).

Table 2 summarizes the results of the C'-subsite SAR, where overall potency was modestly improved by replacing the thiadiazole-based core of **3** with the thiazole-based core of **4**. Heteroaromatic rings such as 3-pyridyl (**5**) and pyrimidine (**6**) yielded an increase in potency with small improvements in selectivity against GluA2 isoforms. Saturated heteroaromatics such as morpholine (**7**) were not as well tolerated. Polar groups such as nitrile (**8**) and various aliphatic alcohols (**9**–**13**) all provided gains in GluN2A potency via displacement and interaction with the C'-subsite water network. In contrast, nonfunctionalized aliphatic groups such as isopropyl (**14**), cyclobutyl (**15**), and cyclopropyl (**16**) did not improve GluN2A potency. However, introduction of π -character via isopropylene (**17**) and a methyl ketone (**18**) brought double digit nanomolar EC₅₀ values, with selectivity against GluA2 receptors reaching greater than 100-fold.

Throughout the SAR exploration at the C'-subsite, we sought to maintain favorable CNS drug-like properties by maintaining P-gp efflux ratios (ERs) less than 3. We were therefore pleased to find that P-gp ERs for compounds **4**–**18** were all less than 2. In addition, we sought to improve selectivity against GluA2 receptors since we believed even low levels of AMPAR potentiation might prove a liability *in vivo*.²² With this in mind, we explored polar groups not normally considered CNS drug-like, such as amides **19** and **20**. The P-gp ERs for these

compounds exceeded our target ratio of 3 due to the increased TPSA and the introduction of hydrogen bond donors, indicating a high likelihood of impaired blood–brain barrier (BBB) penetration *in vivo*, but we were also encouraged by the improved balance of GluN2A potency relative to GluA2 selectivity. In each case, only low levels of AMPAR potentiation were observed at the highest concentrations studied in the assays (125 μ M).

A crystal structure of the methyl amide **19** (Figure 1B) revealed that the amide N–H engages the backbone carbonyl of Pro527 (GluN2A) in a hydrogen bond, enforcing a perpendicular orientation of the amide relative to the core. We hypothesized that the forced perpendicular conformation of amides **19** and **20** was responsible for the observed selectivity against GluA2 receptors, because the amide carbonyl is more likely to clash with the smaller AMPAR pocket. Other features of PAM binding remained the same as previously described for the thiadiazole-based core.

Given the improved potency and selectivity of ethyl amide **20**, we sought to explore SAR at the aniline position, or “right-hand side” (RHS), of the molecules using the crystal structure as a guide in attempts to improve metabolic stability within the series (Table 3). The length of the N-alkyl chain was critical to potency; while the longer propyl chain (**21**) was roughly equipotent with **20**, shorter permutations **22** and **23** were less

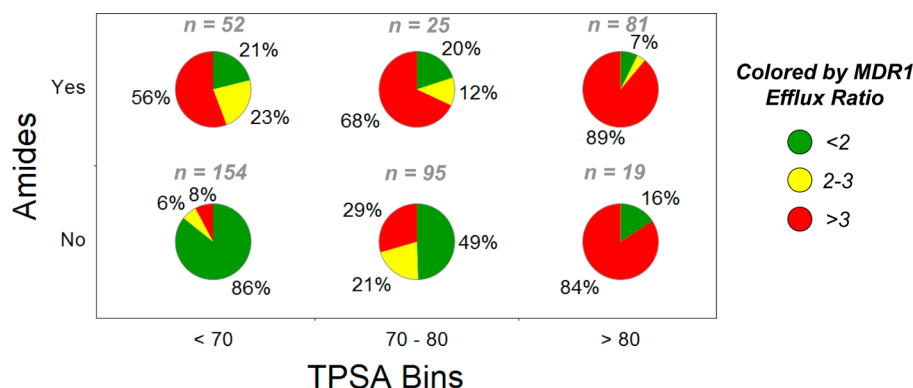


Figure 3. Relationship between MDR1 (P-gp) efflux ratio and TPSA for thiazolopyrimidinone GluN2A PAMs with and without C'-subsite amides.

active. Meanwhile the aminopyridine **24** lost significant potency, without improving metabolic stability relative to the anilines. The ether **25** also lost significant potency ($8.5 \mu\text{M}$) but possessed a notably reduced maximum potentiation (77%) relative to the previously studied *N*-ethyl anilines (typically >140%) and significantly improved *in vitro* liver microsome stability in rodents.

Meta-substituted phenyl groups **26** and **27** possessed micromolar potencies and reduced maximum potentiation. Potency within the phenyl subseries was improved with addition of an ortho-fluorine (**28** and **29**), presumably through increased van der Waals interactions and maximizing the magnitude of the aromatic dipole moment. We hypothesized that this dipole interacted favorably with the antiparallel dipole of the backbone amide of Thr759 (GluN2A) in a π -interaction.²³ Additional SAR within the phenyl and aniline subseries supported this hypothesis (data not shown). Other substitutions on the phenyl ring targeting regions of the binding site occupied by the ethyl group of the anilines (**30** and **31**), as well as methylation of the methylene core linker (**32**), proved unsuccessful at improving GluN2A potency or dramatically impacting maximum potentiation.

We next explored substituted pyrazoles, a heterocycle previously reported in AMPAR PAMs to bind a homologous pocket.²⁴ The 3-trifluoromethyl pyrazole **33** proved a reasonable starting point for our investigations given the modest GluN2A potency and selectivity against AMPARs, while modeling suggested that the 5-position of the pyrazoles provided a suitable vector to explore the pocket occupied by the ethyl group of the anilines. Systematic investigation of functional groups at this site (**34**–**38**) revealed that the chlorine at the 5-position (**35**) possessed a unique balance of GluN2A potency ($0.439 \mu\text{M}$), moderate maximum potentiation (120%), and selectivity against GluA2 receptors (nearly 100-fold selective). Other larger groups, such as the cyclopropyl (**36**) and ethoxy (**37**), reduced AMPAR selectivity and possessed larger maximum potentiation. Meanwhile, attempts to build further into the small pocket off the 5-position, such as isobutoxy analog **38**, proved unproductive.

To better study receptor deactivation kinetics, we developed an automated electrophysiology assay to measure the fold slowing of deactivation in the presence of $100 \mu\text{M}$ PAM; the fold deactivation was defined as the ratio between the inverse deactivation rate constants in the presence of a PAM versus DMSO control. Figure 2A shows the relationship between maximum potentiation (%) and fold deactivation, where various thiazolopyrimidinone-containing PAMs have been

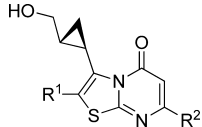
grouped by the identity of the aromatic RHS group, including anilines, pyrazoles, phenyls, and ethers. The plot shows lower maximum potentiation values (40–100%) correlated with deactivation kinetics close to the DMSO control (<3 \times), while higher maximum potentiation values (>150%) resulted in deactivation kinetics 10 \times slower than control. Each aromatic group on the RHS possessed a characteristic deactivation profile; anilines were the slowest deactivating, pyrazoles and phenyls possessed intermediate kinetics, while ethers demonstrated very fast deactivation kinetics. This proved valuable during the SAR and design stage of the program, allowing categorization of the RHS groups according to their deactivation kinetics along with their DMPK properties.

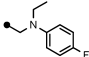
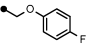
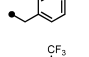
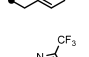
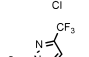
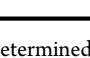
Individual PAMs were studied in greater detail using manual whole-cell patch clamp electrophysiology together with a fast perfusion system. Figure 2B compares the electrophysiology profiles of five amide matched pairs with varying RHS groups including the *N*-ethyl aniline (**20**), ether (**25**), substituted trifluorophenyl (**29**), and substituted trifluoropyrazole (**35**). Notably, the deactivation trends observed for each aromatic group in the automated platform matched the trends in the fast perfusion system (Figure 2A). Each RHS also possessed varying degrees of peak current potentiation, following the same trend as the deactivation kinetics (ether **25** the smallest, aniline **20** the largest).

Crystallographic studies of representative compounds from each RHS subseries (ether **40**, phenyl **29**, pyrazole **49**, and aniline **20**) did not reveal significant structural changes within the LBD that might account for the observed differences in deactivation kinetics. The size and position of the functional group occupying the “floor” of the RHS binding pocket appears to control the deactivation profile of the receptor; ethers (Figure 2C) and phenyls (Figure 2D) without groups in this position possessed the fastest deactivation kinetics, while *N*-chloropyrazole (Figure 2E) and *N*-ethyl anilines (Figure 2F) possessed slower kinetic profiles upon filling this site. Electron withdrawing substituents on each aromatic ring enforce a dipole moment antiparallel to the backbone amide dipole of Thr759 in GluN2A, supporting our design hypothesis that the direction and strength of the ring dipole contributes to GluN2A potency (Figures 2C–F).²³

Studies exploring the efflux properties of a broad set of amide-containing PAMs revealed the difficulty in identifying molecules within this series that are not P-gp substrates (Figure 3). Comparing thiazolopyrimidinone PAMs containing amides in the C'-subsite with those without amides demonstrated the increased probability of P-gp efflux for amides, even at

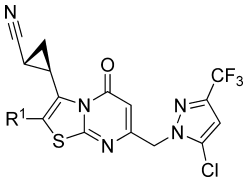
Table 4. Representative Examples of Cyclopropyl Methyl Alcohol SAR



Ex	R ¹	R ²	EC ₅₀ (Max potentiation) ^a μM (%)			LM ^b H/R/M ^c (mL/min/kg)	Hep ^d H/R/M ^c (mL/min/kg)	MDR1 ^e P-gp ER ^f (B:A/A:B) ^g
			GluN2A	GluA2 _{Flip}	GluA2 _{Flop}			
39	•Me		0.0244 (184)	0.870 (84)	0.204 (64)	17 / 48 / 82	ND ⁱ	1.2
40	•Me		0.382 (122)	5.4 (7)	2.3 (6)	7 / 37 / 81	16 / 43 / 74	0.8
41 ^h	•Me		0.90 (160)	32.6 (38)	1.1 (23)	6 / 32 / 77	17 / 41 / 75	3.6
42 ^h	•Me		0.454 (117)	1.7 (57)	0.359 (27)	12 / 38 / 79	ND	0.51
43	•Me		0.0177 (147)	0.150 (85)	0.048 (52)	3 / 32 / 82	15 / 35 / 76	1.3
44	•CF ₃		0.073 (144)	36.1 (66)	2.5 (41)	7 / 20 / 55	15 / 25 / 35	1.0

^aNMDAR EC₅₀ values were determined in the presence of EC₃₀ glutamate and saturating glycine. Max potentiation (%) at 125 μM is reported if no EC₅₀ could be obtained, where 30% denotes the assay baseline (EC₃₀ glutamate). AMPAR EC₅₀ values were determined in the presence of 100 μM glutamate using the AMPA receptor PAM LY450108 as a positive control at 100%. Max potentiation (%) at 125 μM is reported if no EC₅₀ could be obtained, where 0% denotes the assay baseline due to receptor desensitization. All EC₅₀ values represent geometric means of at least two determinations. ^bLiver microsome-predicted hepatic clearance. ^cH/R/M = human/rat/mouse. ^dCryopreserved hepatocyte-predicted hepatic clearance. ^eMDCK-MDR1 human P-gp transfected cell line. ^fEfflux ratio. ^gBasolateral-to-apical/apical-to-basolateral. ^hRacemate. ⁱND = not determined.

Table 5. Representative Examples of Cyclopropyl Nitrile SAR



ex	R ¹	EC ₅₀ (max potentiation), ^a μM (%)			LM ^b H/R/M ^c (mL/min/kg)	Hep ^d H/R/M ^c (mL/min/kg)	MDR1 ^e P-gp ER ^f (B:A/A:B) ^g
		GluN2A	GluA2 _{Flip}	GluA2 _{Flop}			
45	•Me	0.0295 (151)	0.702 (91)	0.073 (93)	5/38/63	5/38/63	5.3
46	•CF ₃	0.021 (152)	9.1 (84)	5.5 (88)	6/8/23	6/8/17	2.1

^aNMDAR EC₅₀ values were determined in the presence of EC₃₀ glutamate and saturating glycine. Max potentiation (%) at 125 μM reported if no EC₅₀ could be obtained, where 30% denotes the assay baseline (EC₃₀ glutamate). AMPAR EC₅₀ values were determined in the presence of 100 μM glutamate using the AMPA receptor PAM LY450108 as a positive control at 100%. Max potentiation (%) at 125 μM reported if no EC₅₀ could be obtained, where 0% denotes the assay baseline due to receptor desensitization. All EC₅₀ values represent geometric means of at least two determinations. ^bLiver microsome-predicted hepatic clearance. ^cH/R/M = human/rat/mouse. ^dCryopreserved hepatocyte-predicted hepatic clearance. ^eMDCK-MDR1 human P-gp transfected cell line. ^fEfflux Ratio. ^gBasolateral-to-apical/apical-to-basolateral.

equivalent TPSAs, due to the added H-bond donor. We recognized that unless the GluN2A potency of the amides could be greatly improved, coverage of the *in vivo* EC₅₀ would be limited due to the observed P-gp efflux. Efforts shifted to identifying GluN2A PAMs outside of the amide subseries that possessed both good selectivity and predicted human pharmacokinetic (PK) properties without P-gp efflux.

Toward this goal, we recognized that the GluN2A potency of various alcohols (9–13) was improved relative to unsubstituted

aliphatic groups (14–16) and that the additional H-bond donor of the alcohol did not introduce P-gp efflux. A key breakthrough came when the conformation of the propyl alcohol 13 was restricted through the addition of a cyclopropyl group to provide *trans*-cyclopropyl methyl alcohol 39 (Table 4). Compound 39 was the most GluN2A-potent PAM on the program to date (24.4 nM) and lacked P-gp efflux but had poor selectivity and metabolic stability. GluN2A potencies of aniline replacements (40–43) were improved in each case relative to

the amide matched pairs (25, 28, 29, and 35) although selectivities against AMPARs were poor, with the exception of ether 40. Compound 40 became a valuable *in vitro* tool compound to explore the properties of a fast-deactivating GluN2A PAM that did not possess any contaminating potentiation of AMPARs. It was later discovered that 40 behaves as a silent allosteric modulator (SAM) at AMPARs, able to bind the receptor but unable to elicit a positive or negative effect on the channel current.¹⁷ Replacement of the core methyl with a trifluoromethyl (44) was found to improve selectivity against AMPARs, without greatly impacting GluN2A potency.

Despite the lack of observed P-gp efflux, all cyclopropyl methyl alcohols remained metabolically labile due to glucuronidation of the primary alcohol as predicted in hepatocytes. As a result, a cyclopropyl methyl alcohol could not be dosed in rodents with sufficient exposures to enable biological evaluation (data not shown). Among the many strategies employed to reduce the metabolic lability of the cyclopropyl methyl alcohol, a cyclopropyl nitrile was explored to maintain polar interactions with the C'-subsite waters, without the risk of glucuronidation. We were pleased to see that the GluN2A potency of *trans*-cyclopropyl nitrile 45 (Table 5) was very similar to the *trans*-cyclopropyl methyl alcohols (30 nM), and that addition of a core trifluoromethyl (GNE-0723, 46) improved both selectivities against AMPARs and metabolic stability without affecting potency (21 nM). Gratifyingly, 46 possessed a rare combination of potency, metabolic stability, and lack of P-gp efflux in a single GluN2A-selective PAM.

A crystal structure of 46 bound to the LBD dimer interface confirmed our design hypothesis. The unique conformation of the *trans*-cyclopropyl allows the nitrile to reach into a distal water-filled pocket off the C'-subsite (Figure 4). Similar to the

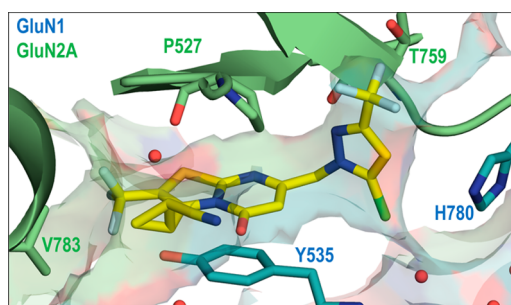


Figure 4. Crystal structure of 46 bound to the GluN1/GluN2A ligand binding domain (PDB code 5I2J). Solvent accessible surface rendering depicts the binding site with relevant amino acids denoted by their single amino acid code. Blue coloring represents residues from GluN1, and green coloring represents residues from GluN2A.

methyl substituent, the trifluoromethyl group interacts with Val783 of GluN2A in a van der Waals interaction, but the source of the improved selectivity against AMPARs is less clear. We believe the selectivity of 46 and related analogs could be derived from the clash of a larger, hydrophobic trifluoromethyl against the more polar serine and asparagine residues of the flip and flop isoforms of GluA2, respectively. A separate small molecule X-ray crystal structure of 46 confirmed the relative and absolute stereochemistry of the 1,2-disubstituted cyclopropyl (see Supporting Information).

Full receptor profiling of 46 against GluN2B/C/D subtypes revealed good selectivity (Figure 5A and Table 6), with a

greater than 250-fold difference between GluN2A and the next most potent glutamate receptor, GluA2_{flop} (Figure 5B and Table 6). Manual electrophysiology demonstrated moderate slowing of deactivation kinetics relative to previously studied PAMs (Figure 5C).

A mouse IV PK study with 46 revealed a good correlation between predicted clearance based on mouse hepatocyte and microsomal stability studies (17 and 23 mL min⁻¹ kg⁻¹, respectively) and *in vivo* clearance (26 mL min⁻¹ kg⁻¹) (Table 6). To support *in vivo* efficacy studies, a mouse PK study explored brain exposure and BBB permeability at a 10 mg/kg PO dose where unbound brain concentrations reached 14 nM at 1 h, compared with unbound plasma concentrations of 17 nM at the same time point. The brain/plasma ratio of these free concentrations at 1 h (0.82) revealed that 46 was BBB permeable, in agreement with the *in vitro* MDCK-MDR1 ER (B:A/A:B = 1.4). This dose was suitable for *in vivo* experiments exploring the bioactivity of 46 in mice, where the GluN2A selective PAM demonstrates promising activity relative to NMDAR antagonists in both locomotor assays and direct measurements of circuit activity using EEG. A detailed account of these studies will be reported in due course.

CHEMISTRY

The syntheses of 1–3 were previously described.¹⁷ The majority of GluN2A PAMs described above were all derived from a common thiazolopyrimidinone core. Depending on the SAR explored, we ideally sought a late-stage functionalization of the vector of interest. Toward this goal, previously described core 47¹⁷ could be treated with *N*-ethyl 4-fluoroaniline to obtain the bromide 48, which was poised for a variety of functionalizations at the C'-subsite (Scheme 1). Standard Suzuki cross-couplings afforded final targets 5, 6, 16, and 17, while copper- and zinc-mediated transformations afforded morpholine 7 and nitrile 8, respectively. Lithiation of 48, followed by quench with ethyl formate, provided aldehyde 49, which could be reduced to provide primary alcohol 7 or treated with methylmagnesium bromide to afford the secondary alcohol 10. A Suzuki cross-coupling afforded enol ether 50, which then set the stage for a hydrolysis/reduction sequence to yield ethyl alcohol 12. Heck coupling between ethyl acrylate and bromide 48 provided enoate 51, which could be fully reduced to propyl alcohol 13.

Other C' subsite analogs could not be easily obtained from bromide 48 and required preinstallation of various functional groups on a precursor aminothiazole (55–58), accessed via α -bromo ketones (52–54). PPA cyclizations afforded alkyl chlorides (59–62), which could be treated with *N*-ethyl 4-fluoroaniline under basic conditions to afford final compounds 4, 14, 15, and 18. Ketone 18 could in turn be transformed into tertiary alcohol 20.

Amide analogs 19–38 were most easily accessed by first forming the aminothiazole amides 64 and 65 and cyclizing directly to the alkyl chlorides 66 and 67 (Scheme 2). Anilines 20–23, aminopyridine 24, and ether 25 were all synthesized by alkylation of the corresponding nucleophiles under basic conditions, while various substituted phenyls 26–31 were formed via palladium-catalyzed Suzuki reactions from the boronic acids. To explore alkylation at the benzylic position adjacent to the phenyl ring, 29 could be treated with excess *n*-butyl lithium and quenched with methyl iodide to yield methylated 32.

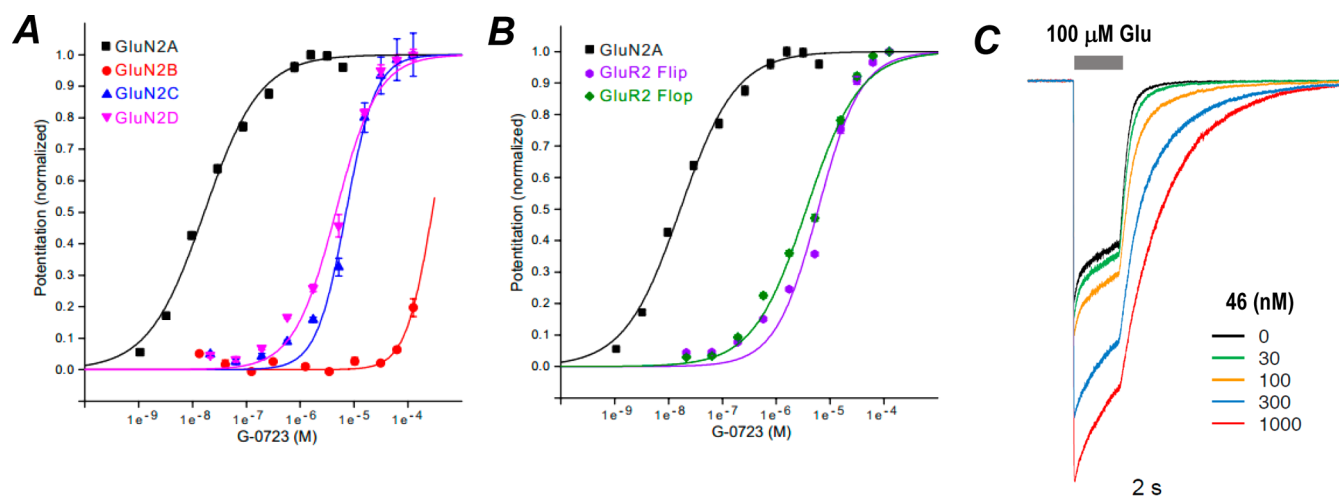


Figure 5. Dose–response curves of **46** comparing (A) GluN2A/2B/2C/2D calcium imaging assays and (B) GluN2A, GluA2_{Flip}, and GluA2_{Flop} calcium imaging assays. (C) Overlay of whole cell voltage clamp recordings comparing deactivation kinetics for **46** at different concentrations.

Table 6. Glutamate Receptor Selectivity and DMPK Summary of **46**

		EC ₅₀ (max potentiation), ^a μM (%)					
GluN2A	GluN2B	GluN2C	GluN2D	GluA2 _{flip}	GluA2 _{flop}		
0.021 (152)	(49)	7.4 (233)	6.2 (160)	9.1 (84)	5.5 (88)		
mouse PK							
in vitro binding		IV (0.3 mg/kg)		PO (10 mg/kg)			
				concentrations at 1 h			
mouse PPB (%)	mouse brain binding (%)	Cl _{blood} (mL min ^{−1} kg ^{−1})	t _{1/2} (h)	F (%)	C _{brain,u} (μM)	C _{plasma,u} (μM)	C _{brain,u} /C _{plasma,u}

^aNMDAR EC₅₀ values were determined in the presence of EC₃₀ glutamate and saturating glycine. Max potentiation (%) at 125 μ M reported if no EC₅₀ could be obtained, where 30% denotes the assay baseline (EC₃₀ glutamate). AMPAR EC₅₀ values were determined in the presence of 100 μ M glutamate using the AMPA receptor PAM LY450108 as a positive control at 100%. Max potentiation (%) at 125 μ M reported if no EC₅₀ could be obtained, where 0% denotes the assay baseline due to receptor desensitization. All EC₅₀ values represent geometric means of at least two determinations.

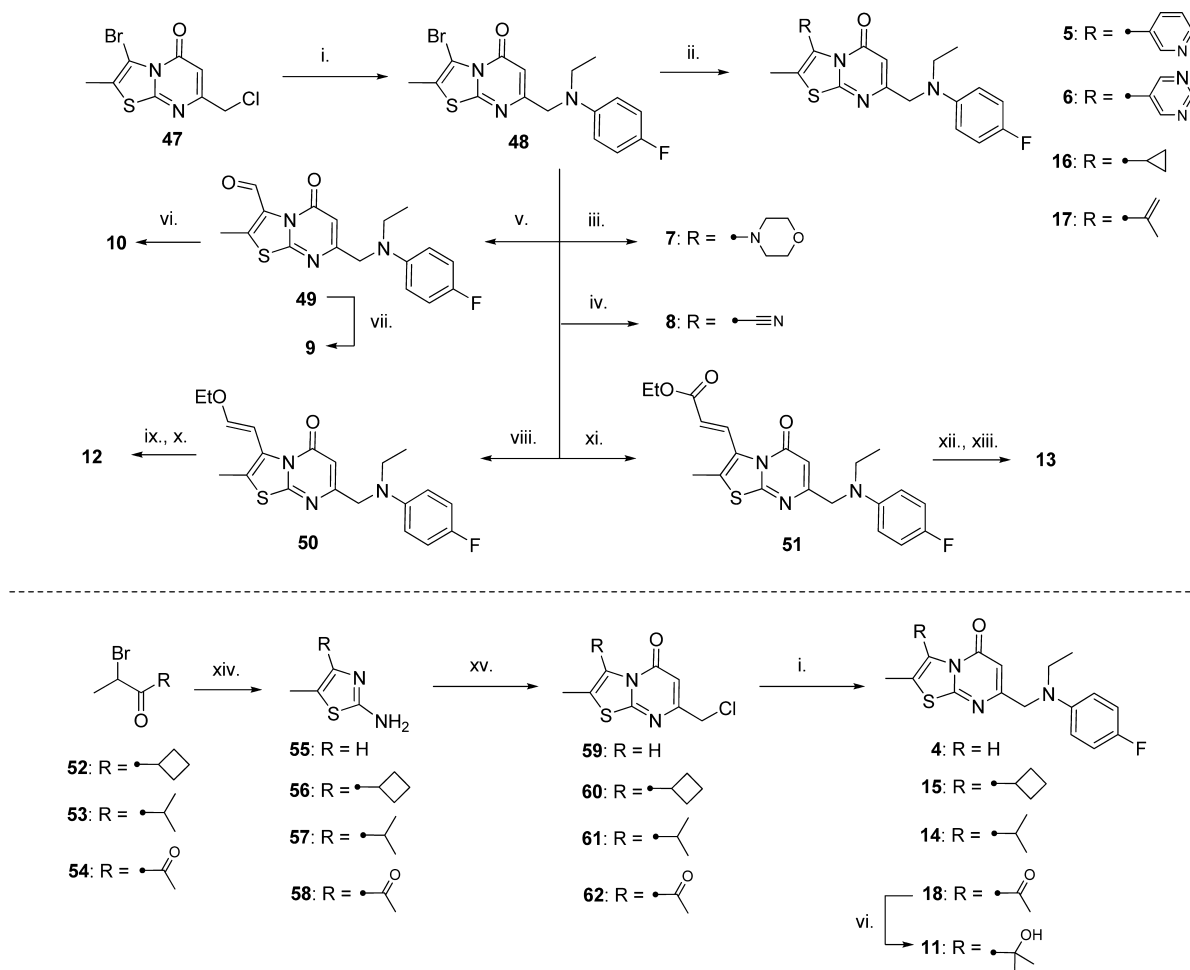
1,5-Substituted pyrazoles were synthesized by two primary methods (Scheme 3). Access to the chloropyrazole **71** was accomplished by first protecting 3-trifluoromethylpyrazole **68** as the *N,N*-dimethyl sulfamoyl **69**, and then selectively deprotonating at the C-5 position with *n*-butyllithium, followed by treatment with hexachloroethane. Chloropyrazole **71** was then obtained by TFA deprotection of sulfamoyl **70**. Other pyrazoles, such as cyclopropylpyrazole **75**, were synthesized by treatment of 1,3-diketones (**74**) with hydrazine hydrate. These pyrazoles could then be easily alkylated by core alkyl chlorides (**67**) using the same methods as *N*-alkyl anilines (Scheme 2) to provide targets **33–38**.

Access to monosubstituted *trans*-cyclopropyls required synthesis of the potassium trifluoroborate building blocks, which were found to perform better in Suzuki cross-coupling reactions relative to the parent pinacol boronate esters (Scheme 4). The *trans*-cyclopropyl methyl alcohol intermediate **78** was accessed from *E*-substituted vinyl boronate ester **76** via Simmons–Smith cyclopropanation using the Shi-modified conditions, providing clean *trans*-cyclopropyl **77**.²⁵ The TBS-protected pinacol boronate ester could then be treated with potassium bifluoride in methanol and water to effect both formation of the potassium trifluoroborate and TBS deprotection toward the final coupling partner **78**. The nitrile **81** was also accessed in two steps (Scheme 4), first borylating cyclopropyl nitrile (**79**) using Hartwig’s iridium catalysis

protocol²⁶ (\rightarrow **80**), followed by the same potassium bifluoride conditions previously described to access the final potassium trifluoroborate **81**.

Most cyclopropyl methyl alcohol analogs in Table 4 were synthesized by first installing the requisite benzylic aromatic group on difunctionalized core **47** using previously described methods, followed by Suzuki cross coupling with the trifluoroborate salt **78** (Scheme 5). Nitrile **45** could be accessed by an analogous method using the cyclopropyl building block **81** (Scheme 4).

The trifluoromethylated core of **44** and **46** required a *de novo* synthesis because the trifluoromethyl group could not be installed on a late-stage intermediate (Scheme 6). Key trifluoromethyl aminothiazole **90** was synthesized beginning from aminothiazole **86**, which was chlorinated using Sandmeyer conditions to provide **87**, because the amine proved detrimental to the key trifluoromethylation event and required protection and removal. Trihalogenated thiazole **88** was generated upon treatment with LDA and elemental iodine after a “halogen dance reaction” at the 4- and 5-positions.²⁷ The three halogens could then be sequentially manipulated, first reacting the iodine under copper-mediated trifluoromethylation conditions to provide trifluoromethyl **89**, followed by regeneration of the amino functionality via condensation with ammonium (\rightarrow **90**). Core formation using previously described PPA conditions then proceeded smoothly to provide alkyl

Scheme 1. Synthesis of C'-Subsite Analogs^a

^aReagents and conditions: (i) *N*-ethyl-4-fluoroaniline, KI, K₂CO₃, MeCN, 70 °C; (ii) R-B(OH)₂, Pd(dppf)Cl₂, Na₂CO₃, MeCN/H₂O, μ wave, 120 °C; (iii) morpholine, L-proline, CuI, K₃PO₄, DMSO, 90 °C; (iv) Zn(CN)₂, Pd₂(dba)₃, dppf, DMF, 160 °C; (v) *n*-BuLi, ethyl formate; (vi) MeMgBr, TFH, rt; (vii) NaBH₄, THF/H₂O, rt; (viii) 2-[(*E*)-2-ethoxyethenyl]-4,4,5,5-tetramethyl-1,3,2-dioxaborolane, Pd(PPh₃)₄, 1,4-dioxane/H₂O, 90 °C; (ix) 3 N HCl, acetone; (x) NaBH₄, MeOH, 0 °C; (xi) ethyl acrylate, Pd₂(dba)₃, P(*o*-Tol)₃, Et₃N, MeCN, 90 °C; (xii) H₂, Pd/C; (xiii) LiBH₄, MeOH; (xiv) thiourea, EtOH; (xv) ethyl 4-chloro-3-oxobutanoate, PPA, 110 °C.

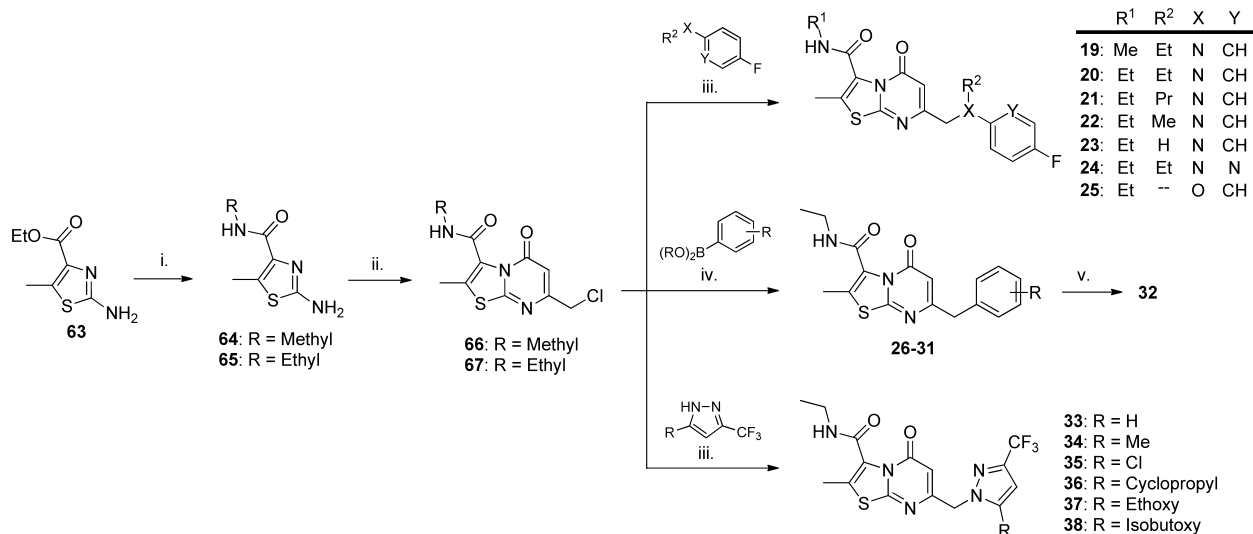
chloride **91**. Pyrazole installation (compound **92**) and final Suzuki cross-coupling using intermediates **78** and **81** provided the final compounds **44** and **46**.

CONCLUSIONS

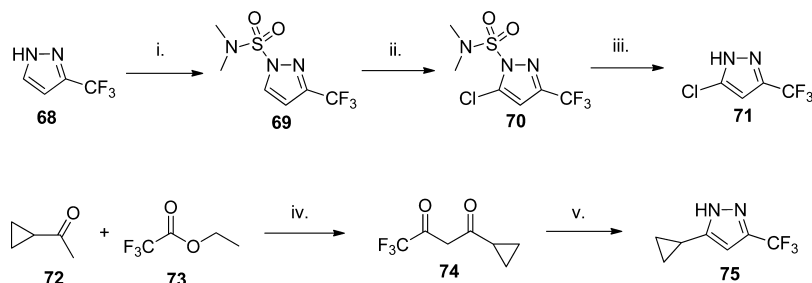
Starting from an optimized HTS hit (**1**), **46** was identified as a potent, GluN2A selective, and BBB penetrable NMDAR PAM suitable for *in vivo* characterization. During the course of this work, we identified the PAM binding site via X-ray crystallography at the dimer interface of the LBD, and using structure-based design, we optimized both potency and kinetics of channel potentiation, characterizing a variety of aromatic groups that can tune channel deactivation kinetics. We also identified a subseries of *trans*-substituted cyclopropyls that provided superior potency within the thiazolopyrimidinone series of PAMs. Upon adding a core trifluoromethyl, we successfully designed a GluN2A-selective PAM suitable for *in vivo* characterization. The results of the *in vivo* studies derived from **46** will be reported in due course.

EXPERIMENTAL SECTION

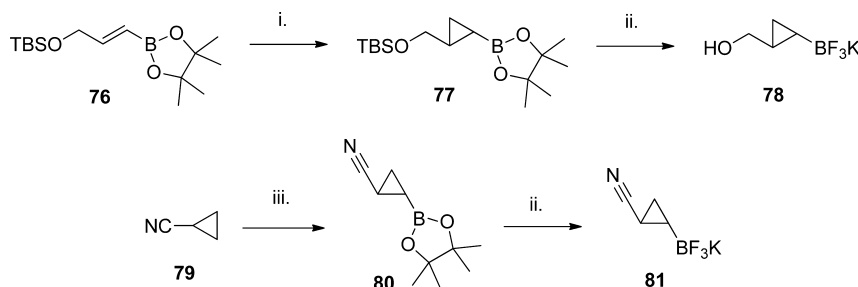
Chemistry. General Methods. Unless otherwise indicated, all commercial reagents and anhydrous solvents were used without additional purification. ¹H-NMR spectra were measured on Bruker Avance III 300, 400, or 500 MHz spectrometers. ¹³C-NMR spectra were measured on a Bruker Avance III 125.80 MHz spectrometer. Chemical shifts (in ppm) were referenced to internal standard tetramethylsilane (δ = 0 ppm). The reported carbon multiplicities and coupling constants are from C–F coupling. High-resolution mass spectrometry of final compounds was performed on a Thermo UHPLC/QE with a Thermo-Q Exactive mass spectrometry detector using ESI ionization, after elution on an Acquity BEH C18 (2.1 mm \times 50 mm; 1.7 μ m particle size) stationary phase using a gradient of water/acetonitrile (3–97% over 7 min; 0.1% formic acid in both phases). Reactions were monitored by walkup Shimadzu LCMS/UV system with LC-30AD solvent pump, 2020 MS, SIL-30AC autosampler, SPD-M30A UV detector, and CTO-20A column oven, using 2–98% acetonitrile/0.1% formic acid (or 0.01% ammonia) over 2.5 min, or by Waters Acquity LCMS system using 2–98% acetonitrile/0.1% formic acid (or 0.1% ammonia) over 2 min. Flash column chromatography purifications were done on a Teledyne Isco Combiflash Rf utilizing Silicycle HP columns. Reverse-phase purification was carried out on a Phenomenex Gemini-NX C18 (30 mm \times 100 mm, 5 μ m) with a gradient of 5–95% acetonitrile/water (with 0.1% formic acid or 0.1%

Scheme 2. Synthesis of Amide Analogs^a

^aReagents and conditions: (i) EtNH₂, EtOH; (ii) ethyl 4-chloro-3-oxobutanoate, PPA, 110 °C; (iii) KI, K₂CO₃, MeCN, 70 °C; (iv) Pd(dppf)Cl₂, Na₂CO₃, 1,4-dioxane/H₂O, 120 °C; (v) *n*-BuLi, MeI, THF.

Scheme 3. Synthesis of 3,5-Substituted Pyrazole Intermediates 71 and 75^a

^aReagents and conditions: (i) *N,N*-dimethylsulfamoyl chloride, DBU, MeCN; (ii) *n*-BuLi, C₂Cl₆, THF; (iii) TFA, DCM; (iv) Na⁰, EtOH; (v) hydrazine hydrate, AcOH, MeOH.

Scheme 4. Synthesis of 1,2-Substituted Cyclopropyl Intermediates 78 and 81^a

^aReagents and conditions: (i) Et₂Zn, TFA, CH₂I₂, DCM; (ii) KHF₂, MeOH/H₂O; (iii) bis(pinacolato) diboron, [Ir(COD)OMe]₂, dimethylphen, THF.

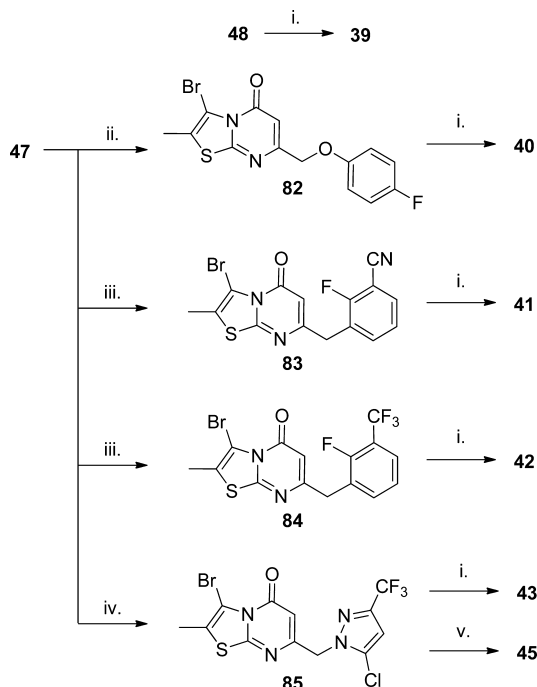
NH₄OH) over 10 min at 60 mL/min. Preparative SFC separations were performed on a PIC Solutions instrument, with conditions indicated in the [Experimental Section](#). Analytical purity was greater than 95% as determined by LCMS using UV 254 nm detection unless stated otherwise. The melting point was determined by differential scanning calorimetry (DSC) (TA Instruments-Waters L.L.C.) by using 5 mg of solid sample and measuring the onset melting temperature.

The syntheses of compounds 1–3 and 47 have been described previously.¹²

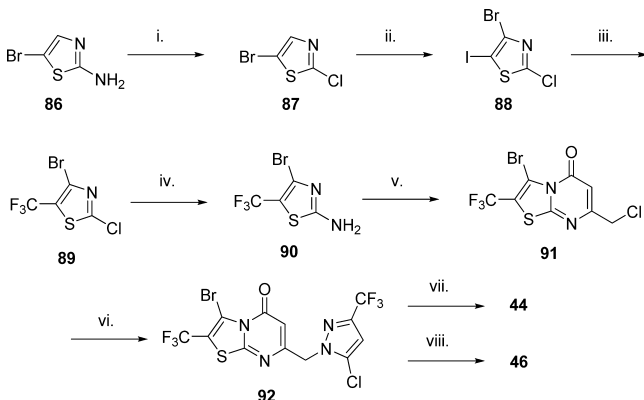
7-((Ethyl(4-fluorophenyl)amino)methyl)-2-methyl-5H-thiazolo[3,2-*a*]pyrimidin-5-one (4). The title compound was prepared in a manner analogous to 15 (29% yield, 2 steps). HRMS (ESI) Calcd for

C₁₆H₁₇FN₃OS (M + H)⁺: 318.1071. Found: 318.1079. ¹H NMR (400 MHz, DMSO-*d*₆) δ 7.84 (d, *J* = 1.8 Hz, 1H), 7.03–6.92 (m, 2H), 6.66–6.56 (m, 2H), 5.93 (s, 1H), 4.35 (s, 2H), 3.47 (q, *J* = 7.0 Hz, 2H), 2.42 (d, *J* = 1.4 Hz, 3H), 1.13 (t, *J* = 7.0 Hz, 3H).

7-((Ethyl(4-fluorophenyl)amino)methyl)-2-methyl-3-(pyridin-3-yl)-5H-thiazolo[3,2-*a*]pyrimidin-5-one (5). The title compound was prepared from bromide 48 in a manner analogous to 6 (52% yield). HRMS (ESI) Calcd for C₂₁H₂₀FN₄OS (M + H)⁺: 395.1336. Found: 396.1347. ¹H NMR (400 MHz, DMSO-*d*₆) δ 8.57 (d, *J* = 5.0 Hz, 1H), 8.54 (d, *J* = 2.1 Hz, 1H), 7.78 (dd, *J* = 7.9, 1.9 Hz, 1H), 7.42 (dd, *J* = 7.9, 5.0 Hz, 1H), 6.98 (t, *J* = 8.8 Hz, 2H), 6.62 (dd, *J* = 9.1, 4.4 Hz,

Scheme 5. Synthesis of Cyclopropyl Analogs 39–43 and 45^a

^aReagents and conditions: (i) **76**, Pd(dppf)Cl₂, Na₂CO₃, 1,4-dioxane/H₂O, 120 °C; (ii) 4-fluorophenol, KI, K₂CO₃, MeCN, 70 °C; (iii) ArB(OH)₂, Pd(dppf)Cl₂, Na₂CO₃, 1,4-dioxane/H₂O, 120 °C; (iv) **69**, KI, K₂CO₃, MeCN, 70 °C; (v) **79**, Pd(dppf)Cl₂, Na₂CO₃, 1,4-dioxane/H₂O, 85 °C.

Scheme 6. Synthesis of Trifluoromethyl Analogs 44 and 46^a

^aReagents and conditions: (i) *t*-BuONO, CuCl, MeCN, then H₂O; (ii) LDA, I₂, THF; (iii) 2,2-difluoro-2-(fluorosulfonyl)acetate, CuI, DMF, 80 °C; (iv) NH₃/H₂O, 1,4-dioxane, 50 °C; (v) ethyl 4-chloro-3-oxobutanoate, PPA, 130 °C; (vi) **69**, Na₂CO₃, MeCN, 80 °C; (vii) **76**, Pd(dppf)Cl₂, Na₂CO₃, 1,4-dioxane/H₂O, 120 °C; (viii) **79**, Pd(dppf)Cl₂, Na₂CO₃, 1,4-dioxane/H₂O, 85 °C.

2H), 5.81 (s, 1H), 4.35 (s, 2H), 3.47 (q, *J* = 7.0 Hz, 2H), 2.16 (s, 3H), 1.13 (t, *J* = 7.0 Hz, 3H).

7-((Ethyl(4-fluorophenyl)amino)methyl)-2-methyl-3-(pyrimidin-5-yl)-5H-thiazolo[3,2-*a*]pyrimidin-5-one (6). To a solution of bromide **48** (50 mg, 0.13 mmol) in acetonitrile/H₂O (1.3/0.5 mL) was added (pyrimidin-5-yl)boronic acid (20.3 mg, 0.16 mmol), sodium carbonate (40.5 mg, 0.379 mmol), and [1,1'-bis(diphenylphosphino)-ferrocene]palladium(II) dichloride (9.7 mg, 0.013 mmol). The reaction mixture was heated under microwave irradiation for 20 min at 120 °C. After cooling to room temperature, the resulting mixture was concentrated *in vacuo*. The residue was purified by silica gel

chromatography with dichloromethane/methanol (95/5) to afford the title compound (14.8 mg, 30.0%) as an off-white solid. HRMS (ESI) Calcd for C₂₀H₁₉FN₃O₂S (M + H)⁺: 396.1289. Found: 396.1303. ¹H NMR (400 MHz, DMSO-*d*₆) δ 9.18 (s, 1H), 8.83 (s, 2H), 6.98 (t, *J* = 8.8 Hz, 2H), 6.62 (dd, *J* = 9.2, 4.4 Hz, 2H), 5.85 (s, 1H), 4.36 (s, 2H), 3.47 (q, *J* = 7.0 Hz, 2H), 2.22 (s, 3H), 1.13 (t, *J* = 7.0 Hz, 3H).

7-((Ethyl(4-fluorophenyl)amino)methyl)-2-methyl-3-morpholino-5H-thiazolo[3,2-*a*]pyrimidin-5-one (7). To a solution of bromide **48** (250 mg, 0.63 mmol) in dimethyl sulfoxide (3 mL) was added potassium phosphate (268 mg, 1.26 mmol), L-proline (22.0 mg, 0.19 mmol), morpholine (165 mg, 1.89 mmol), and cuprous iodide (18.0 mg, 0.09 mmol), and the reaction mixture was stirred overnight at 90 °C. The resulting mixture was then quenched with water (50 mL), extracted with ethyl acetate (30 mL × 3), washed with brine, dried over anhydrous sodium sulfate, and concentrated *in vacuo*. The residue was purified by chromatography with ethyl acetate/petroleum ether (1/2) to afford the title compound (29.5 mg, 12%) as a white solid. HRMS (ESI) Calcd for C₂₀H₂₄FN₄O₂S (M + H)⁺: 403.1599. Found: 403.1608. ¹H NMR (300 MHz, CDCl₃) δ 6.93–6.87 (m, 2H), 6.61–6.57 (m, 2H), 6.15 (s, 1H), 4.29 (s, 2H), 3.91–3.87 (m, 2H), 3.76–3.59 (m, 4H), 3.50–3.43 (m, 2H), 2.64–2.60 (m, 2H), 2.40 (s, 3H), 1.25–1.20 (m, 3H).

7-((Ethyl(4-fluorophenyl)amino)methyl)-2-methyl-5-oxo-5H-thiazolo[3,2-*a*]pyrimidine-3-carbonitrile (8). To a solution of bromide **48** (1 g, 2.523 mmol) in DMF (5 mL) was added zinc cyanide (605 mg, 5.05 mmol), tris(dibenzylideneacetone)dipalladium(0) (118 mg, 0.126 mmol), and dppf (143 mg, 0.2523 mmol). The reaction mixture was then heated at 160 °C overnight. The resulting mixture was then quenched with water (500 mL), extracted with ethyl acetate (300 mL × 3), washed with brine, dried over anhydrous sodium sulfate, and concentrated *in vacuo*. The residue was purified by silica gel chromatography using ethyl acetate/heptane (0–100% ethyl acetate gradient) to afford the title compound (284 mg, 33%) as a white solid. HRMS (ESI) Calcd for C₁₇H₁₆FN₄O₂S (M + H)⁺: 343.1023. Found: 343.1031. ¹H NMR (400 MHz, DMSO-*d*₆) δ 6.98 (t, *J* = 8.7 Hz, 2H), 6.62 (dd, *J* = 9.1, 4.4 Hz, 2H), 6.01 (s, 1H), 4.36 (s, 2H), 3.47 (q, *J* = 7.0 Hz, 2H), 2.60 (s, 3H), 1.13 (t, *J* = 6.9 Hz, 3H).

7-((Ethyl(4-fluorophenyl)amino)methyl)-3-(hydroxymethyl)-2-methyl-5H-thiazolo[3,2-*a*]pyrimidin-5-one (9). To a solution of aldehyde **49** (100 mg, 0.29 mmol) in tetrahydrofuran (10 mL) was added water (2 mL) and sodium borohydride (33 mg, 0.87 mmol). The reaction mixture was stirred overnight at room temperature and then quenched with water (50 mL). The resulting solution was extracted with ethyl acetate (30 mL × 3), washed with brine, dried over anhydrous sodium sulfate, and concentrated *in vacuo*. The residue was purified by chromatography with 50% ethyl acetate in petroleum ether to afford the title compound (60 mg, 60%) as an off-white solid. HRMS (ESI) Calcd for C₁₇H₁₉FN₃O₂S (M + H)⁺: 348.1177. Found: 348.1188. ¹H NMR (300 MHz, CDCl₃) δ 6.93–6.86 (m, 2H), 6.59–6.54 (m, 2H), 6.26 (s, 1H), 4.75–4.73 (m, 2H), 4.49–4.44 (m, 1H), 4.32 (s, 2H), 3.48 (q, *J* = 6.9 Hz, 2H), 2.44 (s, 3H), 1.23 (t, *J* = 6.9 Hz, 3H).

7-((Ethyl(4-fluorophenyl)amino)methyl)-3-(1-hydroxyethyl)-2-methyl-5H-thiazolo[3,2-*a*]pyrimidin-5-one (10). To a solution of aldehyde **49** (200 mg, 0.58 mmol) in tetrahydrofuran (15 mL) was added methylmagnesium bromide (1.3 mL, 0.5 mol/L). The resulting solution was stirred overnight at room temperature. The reaction was then quenched by saturated ammonium chloride (20 mL), extracted with dichloromethane (3 × 30 mL), washed with brine, dried over sodium sulfate, and concentrated *in vacuo*. The residue was purified by chromatography with ethyl acetate/petroleum ether (1/2) to afford the title compound (67.5 mg, 31%) as an off-white solid. HRMS (ESI) Calcd for C₁₈H₂₁FN₃O₂S (M + H)⁺: 362.1333. Found: 362.1341. ¹H NMR (300 MHz, CD₃OD) δ 6.95–6.88 (m, 2H), 6.71–6.65 (m, 2H), 6.20 (s, 1H), 5.43–5.36 (m, 1H), 4.39 (s, 2H), 3.53 (q, *J* = 7.2 Hz, 2H), 2.50 (s, 3H), 1.52 (d, *J* = 6.6 Hz, 3H), 1.22 (t, *J* = 7.2 Hz, 3H).

7-((Ethyl(4-fluorophenyl)amino)methyl)-3-(2-hydroxypropan-2-yl)-2-methyl-5H-thiazolo[3,2-*a*]pyrimidin-5-one (11). To a solution of ketone **18** (70 mg, 0.19 mmol) in tetrahydrofuran (15 mL) was

added methylmagnesium bromide in tetrahydrofuran (1 mol/L, 0.42 mL). The reaction was stirred for 48 h at room temperature and was then quenched by a saturated aqueous ammonium chloride solution (20 mL). The resulting mixture was then extracted with dichloromethane (3 × 30 mL), washed with brine, dried over anhydrous sodium sulfate, and concentrated *in vacuo*. The residue was purified by chromatography with dichloromethane/methanol (50/1) to afford the title compound (40 mg, 52%) as a yellow solid. HRMS (ESI) Calcd for $C_{19}H_{23}FN_3O_2S$ ($M + H$)⁺: 376.1490. Found: 376.1501. ¹H NMR (300 MHz, CD_3OD) δ 6.95–6.89 (m, 2H), 6.70–6.65 (m, 2H), 6.24 (s, 1H), 4.39 (s, 2H), 3.53 (q, $J = 6.9$ Hz, 2H), 2.58 (s, 3H), 1.73 (s, 6H), 1.23 (t, $J = 6.9$ Hz, 3H).

7-((Ethyl(4-fluorophenyl)amino)methyl)-3-(2-hydroxyethyl)-2-methyl-5H-thiazolo[3,2-a]pyrimidin-5-one (12). To a solution of enol ether **50** (250 mg, 0.65 mmol) in acetone was added 3 N hydrogen chloride (15 mL). The resulting solution was refluxed for 3 h in an oil bath. The pH value of the solution was then adjusted to pH 8 with a saturated aqueous sodium bicarbonate solution. The mixture was extracted with dichloromethane (3 × 50 mL), washed with brine, dried over anhydrous sodium sulfate, and concentrated *in vacuo* to afford the title compound as a light yellow oil (180 mg). The crude aldehyde product was used in the next step without further purification.

To a solution of the crude aldehyde (180 mg, 0.50 mmol) in methanol (10 mL) was added sodium borohydride (40 mg, 1.06 mmol) at 0 °C. After stirring overnight at room temperature, the reaction was quenched by saturated aqueous ammonium chloride (20 mL). The resulting solution was extracted with dichloromethane (3 × 50 mL), washed with brine, dried over anhydrous sodium sulfate, and concentrated *in vacuo*. The residue was purified by chromatography with dichloromethane/methanol (30/1) to afford the title compound (90 mg, 38% yield, 2 steps) as a white solid. HRMS (ESI) Calcd for $C_{18}H_{21}FN_3O_2S$ ($M + H$)⁺: 362.1333. Found: 362.1342. ¹H NMR (300 MHz, $CDCl_3$) δ 6.90–6.84 (m, 2H), 6.55–6.50 (m, 2H), 6.14 (s, 1H), 4.26 (s, 2H), 3.89–3.85 (m, 2H), 3.47–3.39 (m, 4H), 2.95–2.91 (m, 1H), 2.32 (s, 3H), 1.19 (t, $J = 6.9$ Hz, 3H).

7-((Ethyl(4-fluorophenyl)amino)methyl)-3-(3-hydroxypropyl)-2-methyl-5H-thiazolo[3,2-a]pyrimidin-5-one (13). To a solution of enoate **51** (200 mg, 0.5 mmol) in methanol (10 mL) was added 10% palladium on carbon, and the reaction solution was stirred 12 h at room temperature under a hydrogen atmosphere (1.5 atm). After filtration, the resulting solution was concentrated *in vacuo* to afford the title compound (180 mg, 90%) as a light yellow solid. HRMS (ESI) Calcd for $C_{19}H_{23}FN_3O_2S$ ($M + H$)⁺: 376.1490. Found: 376.1500. ¹H NMR (300 MHz, $CDCl_3$) δ 6.94–6.88 (m, 2H), 6.62–6.58 (m, 2H), 6.12 (s, 1H), 4.28 (s, 2H), 4.11 (q, $J = 7.2$ Hz, 2H), 3.51–3.41 (m, 4H), 2.73 (t, $J = 6.9$ Hz, 2H), 2.37 (s, 3H), 1.26–1.20 (m, 6H).

To a solution of ethyl ester from the previous step (180 mg, 0.43 mmol) in methanol (10 mL) was added lithium borohydride (20 mg, 0.91 mmol) at 0 °C. The resulting solution was stirred for 5 h at room temperature. The reaction was then quenched by a saturated aqueous ammonium chloride solution (20 mL), extracted with dichloromethane (3 × 50 mL), washed with brine, dried over anhydrous sodium sulfate, and then concentrated *in vacuo*. The residue was purified by silica gel chromatography with dichloromethane/methanol (30/1) to afford the title compound (100 mg, 62%) as a light yellow solid. LCMS, $m/z = 376.0$ [$M + H$]⁺. ¹H NMR (400 MHz, $CDCl_3$) δ 6.94–6.90 (m, 2H), 6.63–6.59 (m, 2H), 6.15 (s, 1H), 4.30 (s, 2H), 3.67 (t, $J = 5.6$ Hz, 2H), 3.48 (q, $J = 7.2$ Hz, 2H), 3.33 (t, $J = 7.2$ Hz, 2H), 2.36 (s, 3H), 1.90–1.95 (m, 2H), 1.20 (t, $J = 7.2$ Hz, 3H).

7-((Ethyl(4-fluorophenyl)amino)methyl)-3-isopropyl-2-methyl-5H-thiazolo[3,2-a]pyrimidin-5-one (14). The title compound was prepared in a manner analogous to **15** (6% yield, 2 steps). LCMS, $m/z = 360.0$ [$M + H$]⁺. ¹H NMR (300 MHz, CD_3OD) δ 6.95–6.86 (m, 2H), 6.19–6.69 (m, 2H), 6.05 (s, 1H), 4.33 (s, 2H), 3.53 (q, $J = 6.9$ Hz, 2H), 2.44 (s, 3H), 2.10 (m, 1H), 1.40 (d, $J = 7.2$ Hz, 6H), 1.21 (t, $J = 6.9$ Hz, 3H).

3-Cyclobutyl-7-((ethyl(4-fluorophenyl)amino)methyl)-2-methyl-5H-thiazolo[3,2-a]pyrimidin-5-one (15). To a solution of alkyl chloride **60** (300 mg, 1.12 mmol) in acetonitrile (20 mL) was

added potassium iodide (93 mg, 0.56 mmol), potassium carbonate (309 mg, 2.24 mmol), and *N*-ethyl-4-fluoroaniline (311 mg, 2.23 mmol). The resulting solution was stirred for 5 h at 70 °C. After concentration *in vacuo*, the crude product was purified by Prep-HPLC with the following conditions (Agilent 1200; column, X-Brigde C18; mobile phase, 0.05% NH_4HCO_3 in water and CH_3CN (CH_3CN 20% up to 60% in 15 min); detector, UV254) to afford the title compound (36.1 mg, 8%) as a yellow solid. HRMS (ESI) Calcd for $C_{20}H_{23}FN_3OS$ ($M + H$)⁺: 372.1540. Found: 372.1553. ¹H NMR (300 MHz, CD_3OD) δ 6.93–6.86 (m, 2H), 6.69–6.62 (m, 2H), 6.01 (s, 1H), 4.44–4.35 (m, 1H), 4.31 (s, 2H), 3.51 (q, $J = 6.9$ Hz, 2H), 2.48 (s, 3H), 2.45–2.35 (m, 3H), 1.89–1.890 (m, 1H), 2.06–1.94 (m, 1H), 1.21 (t, $J = 6.9$ Hz, 3H).

3-Cyclopropyl-7-((ethyl(4-fluorophenyl)amino)methyl)-2-methyl-5H-thiazolo[3,2-a]pyrimidin-5-one (16). The title compound was prepared from bromide **48** in a manner analogous to **6** (31% yield). HRMS (ESI) Calcd for $C_{19}H_{21}FN_3OS$ ($M + H$)⁺: 358.1384. Found: 358.1393. ¹H NMR (400 MHz, $DMSO-d_6$) δ 6.98 (t, $J = 8.7$ Hz, 2H), 6.61 (dd, $J = 9.2, 4.3$ Hz, 2H), 5.82 (s, 1H), 4.29 (s, 2H), 3.46 (q, $J = 7.0$ Hz, 2H), 2.34 (s, 3H), 2.14 (p, $J = 7.6$ Hz, 1H), 1.12 (t, $J = 7.0$ Hz, 3H), 0.92 (t, $J = 7.1$ Hz, 2H), 0.66 (t, $J = 5.6$ Hz, 2H).

7-((Ethyl(4-fluorophenyl)amino)methyl)-2-methyl-3-(prop-1-en-2-yl)-5H-thiazolo[3,2-a]pyrimidin-5-one (17). The title compound was prepared from bromide **48** in a manner analogous to **6** (62% yield). LCMS, $m/z = 358.1$ [$M + H$]⁺. ¹H NMR (400 MHz, $DMSO-d_6$) δ 6.98 (t, $J = 8.6$ Hz, 2H), 6.61 (dd, $J = 9.0, 4.3$ Hz, 2H), 5.86 (s, 1H), 5.35 (s, 1H), 5.00 (s, 1H), 4.33 (s, 2H), 3.47 (q, $J = 7.0$ Hz, 2H), 2.28 (s, 3H), 1.94 (s, 3H), 1.13 (t, $J = 7.0$ Hz, 3H).

3-Acetyl-7-((ethyl(4-fluorophenyl)amino)methyl)-2-methyl-5H-thiazolo[3,2-a]pyrimidin-5-one (18). The title compound was prepared in a manner analogous to **15** (3% yield, 3 steps). HRMS (ESI) Calcd for $C_{18}H_{19}FN_3O_2S$ ($M + H$)⁺: 360.1177. Found: 360.1186. ¹H NMR (300 MHz, CD_3OD) δ 6.95–6.89 (m, 2H), 6.70–6.65 (m, 2H), 6.16 (s, 1H), 4.40 (s, 2H), 3.53 (q, $J = 7.4$ Hz, 2H), 2.42 (s, 3H), 2.39 (s, 3H), 1.23 (t, $J = 7.4$ Hz, 3H).

7-((Ethyl(4-fluorophenyl)amino)methyl)-*N*,2-dimethyl-5-oxo-5H-thiazolo[3,2-a]pyrimidine-3-carboxamide (19). The title compound was prepared from chloride **66** in a manner analogous to **48** (64% yield). HRMS (ESI) Calcd for $C_{18}H_{20}FN_4O_2S$ ($M + H$)⁺: 375.1286. Found: 375.1298. ¹H NMR (300 MHz, $DMSO-d_6$) δ 8.36–8.37 (m, 1H), 6.95–7.14 (m, 2H), 6.59–6.68 (m, 2H), 5.90 (s, 1H), 4.42 (s, 2H), 3.35–3.48 (q, $J = 6.9$ Hz, 2H), 2.72 (d, $J = 4.8$ Hz, 3H), 2.30 (s, 3H), 1.12 (t, $J = 6.9$ Hz, 3H).

***N*-Ethyl-7-((ethyl(4-fluorophenyl)amino)methyl)-2-methyl-5-oxo-5H-thiazolo[3,2-a]pyrimidine-3-carboxamide (20).** The title compound was prepared from chloride **67** in a manner analogous to **48** (80% yield). HRMS (ESI) Calcd for $C_{19}H_{22}FN_4O_2S$ ($M + H$)⁺: 389.1442. Found: 389.1451. ¹H NMR (400 MHz, $CDCl_3$) δ 6.93–6.85 (m, 2H), 6.61–6.56 (m, 2H), 6.18 (s, 1H), 6.00–5.97 (m, 1H), 4.30 (s, 2H), 3.55–3.42 (m, 4H), 2.39 (s, 3H), 1.29–1.18 (m, 6H).

***N*-Ethyl-7-(((4-fluorophenyl)(propyl)amino)methyl)-2-methyl-5-oxo-5H-thiazolo[3,2-a]pyrimidine-3-carboxamide (21).** The title compound was prepared from chloride **67** in a manner analogous to **48** (71% yield). HRMS (ESI) Calcd for $C_{20}H_{24}FN_4O_2S$ ($M + H$)⁺: 403.1599. Found: 403.1609. ¹H NMR (400 MHz, $DMSO-d_6$) δ 8.42 (t, $J = 5.6$ Hz, 1H), 6.96–6.85 (m, 2H), 6.60–6.49 (m, 2H), 6.27 (t, $J = 6.3$ Hz, 1H), 6.10 (s, 1H), 4.14 (d, $J = 6.3$ Hz, 2H), 3.22 (qd, $J = 7.2, 5.5$ Hz, 2H), 2.31 (s, 3H), 1.09 (t, $J = 7.2$ Hz, 3H).

***N*-Ethyl-7-(((4-fluorophenyl)(methyl)amino)methyl)-2-methyl-5-oxo-5H-thiazolo[3,2-a]pyrimidine-3-carboxamide (22).** The title compound was prepared from chloride **67** in a manner analogous to **48** (30% yield). HRMS (ESI) Calcd for $C_{18}H_{20}FN_4O_2S$ ($M + H$)⁺: 375.1286. Found: 375.1296. ¹H NMR (400 MHz, $DMSO-d_6$) δ 8.41 (t, $J = 5.6$ Hz, 1H), 7.06–6.94 (m, 2H), 6.73–6.61 (m, 2H), 5.87 (s, 1H), 4.41 (s, 2H), 3.21 (qd, $J = 7.2, 5.5$ Hz, 2H), 3.05 (s, 3H), 2.31 (s, 3H), 1.08 (t, $J = 7.2$ Hz, 3H).

***N*-Ethyl-7-((4-fluorophenylamino)methyl)-2-methyl-5-oxo-5H-thiazolo[3,2-a]pyrimidine-3-carboxamide (23).** The title compound was prepared from chloride **67** in a manner analogous to **48** (38% yield). HRMS (ESI) Calcd for $C_{17}H_{18}FN_4O_2S$ ($M + H$)⁺: 361.1129. Found: 361.1139. ¹H NMR (400 MHz, $DMSO-d_6$) δ 8.42 (t, $J = 5.6$

Hz, 1H), 6.96–6.85 (m, 2H), 6.60–6.49 (m, 2H), 6.27 (t, $J = 6.3$ Hz, 1H), 6.10 (s, 1H), 4.14 (d, $J = 6.3$ Hz, 2H), 3.22 (qd, $J = 7.2, 5.5$ Hz, 2H), 2.31 (s, 3H), 1.09 (t, $J = 7.2$ Hz, 3H).

N-Ethyl-7-((ethyl(5-fluoropyridin-2-yl)amino)methyl)-2-methyl-5-oxo-5H-thiazolo[3,2-a]pyrimidine-3-carboxamide (24). The title compound was prepared from chloride **67** in a manner analogous to **48** (24% yield). HRMS (ESI) Calcd for $C_{18}H_{21}FN_5O_2S$ ($M + H$)⁺: 390.1395. Found: 390.1402. ¹H NMR (400 MHz, DMSO-*d*₆) δ 8.40 (t, $J = 5.5$ Hz, 1H), 8.02 (d, $J = 3.2$ Hz, 1H), 6.69–6.61 (m, 1H), 5.85 (s, 1H), 4.54 (s, 2H), 3.58 (q, $J = 6.9$ Hz, 2H), 3.22 (qd, $J = 7.3, 5.5$ Hz, 2H), 2.31 (s, 3H), 1.11 (dt, $J = 20.4, 7.1$ Hz, 6H).

N-Ethyl-7-((4-fluorophenoxy)methyl)-2-methyl-5-oxo-5H-thiazolo[3,2-a]pyrimidine-3-carboxamide (25). The title compound was prepared from chloride **67** in a manner analogous to **48** (22% yield). HRMS (ESI) Calcd for $C_{17}H_{17}FN_3O_3S$ ($M + H$)⁺: 362.0969. Found: 362.0980. ¹H NMR (300 MHz, CDCl₃) δ 7.00–6.96 (m, 2H), 6.90–6.86 (m, 2H), 6.45 (s, 1H), 5.89 (s, 1H), 4.91 (s, 2H), 3.57–3.51 (m, 2H), 2.42 (s, 3H), 1.29 (t, $J = 7.2$ Hz, 3H).

7-(3-Cyanobenzyl)-N-ethyl-2-methyl-5-oxo-5H-thiazolo[3,2-a]pyrimidine-3-carboxamide (26). The title compound was prepared from chloride **67** in a manner analogous to **28** (31% yield). HRMS (ESI) Calcd for $C_{18}H_{17}N_4O_2S$ ($M + H$)⁺: 353.1067. Found: 353.1078. ¹H NMR (400 MHz, CDCl₃) δ 7.56–7.48 (m, 3H), 7.44–7.40 (m, 1H), 6.07 (s, 1H), 5.83 (s, 1H), 3.90 (s, 2H), 3.56–3.49 (m, 2H), 2.42 (s, 3H), 1.28 (t, $J = 7$ Hz, 3H).

N-Ethyl-2-methyl-5-oxo-7-(3-(trifluoromethyl)benzyl)-5H-thiazolo[3,2-a]pyrimidine-3-carboxamide (27). The title compound was prepared from chloride **67** in a manner analogous to **28** (20% yield). HRMS (ESI) Calcd for $C_{18}H_{17}F_3N_3O_2S$ ($M + H$)⁺: 396.0988. Found: 396.0996. ¹H NMR (300 MHz, CDCl₃) δ 7.51–7.50 (m, 2H), 7.45–7.43 (m, 2H), 6.06 (s, 1H), 5.81–5.77 (m, 1H), 3.93 (s, 2H), 3.57–3.48 (m, 2H), 2.41 (s, 3H), 1.28 (m, 3H).

7-(3-Cyano-2-fluorobenzyl)-N-ethyl-2-methyl-5-oxo-5H-thiazolo[3,2-a]pyrimidine-3-carboxamide (28). To a solution of alkyl chloride **67** (500 mg, 1.75 mmol) in 1,4-dioxane/H₂O (10/3 mL) was added sodium carbonate (370 mg, 3.49 mmol), Pd(dppf)Cl₂ (127 mg, 0.170 mmol), and 3-cyano-2-fluorophenylboronic acid (578 mg, 3.50 mmol). The reaction mixture was then stirred for 30 min at 120 °C. After concentration under vacuum, the residue was purified on silica gel column with dichloromethane/methanol (50/1) to afford the title compound (0.56 g, 75%) as an off-white solid. Mp 191 °C. HRMS (ESI) Calcd for $C_{18}H_{16}O_2N_4FS$ ($M + H$)⁺: 371.0973. Found: 371.0986. ¹H NMR (500 MHz, DMSO-*d*₆) δ 8.41 (t, $J = 5.5$ Hz, 1H), 7.85 (ddd, $J = 1.8, 6.1, 7.7$ Hz, 1H), 7.76 (ddd, $J = 1.8, 7.7, 7.7$ Hz, 1H), 7.39 (dd, $J = 7.7, 7.7$ Hz, 1H), 6.14 (s, 1H), 4.01 (s, 2H), 3.23 (qd, $J = 5.6, 7.2$ Hz, 2H), 2.30 (s, 3H), 1.10 (t, $J = 7.2$ Hz, 3H). ¹³C NMR (126 MHz, DMSO) δ 162.23, 161.67, 160.65 (d, $J_{CF} = 254.8$ Hz), 158.37, 157.04, 137.38 (d, $J_{CF} = 5.3$ Hz), 132.48, 128.52, 126.20 (d, $J_{CF} = 14.3$ Hz), 125.43 (d, $J_{CF} = 3.8$ Hz), 122.58, 113.99, 104.50, 100.12 (d, $J_{CF} = 14.8$ Hz), 35.13, 33.92, 14.11, 11.42.

N-Ethyl-7-(2-fluoro-3-(trifluoromethyl)benzyl)-2-methyl-5-oxo-5H-thiazolo[3,2-a]pyrimidine-3-carboxamide (29). The title compound was prepared from chloride **67** in a manner analogous to **28** (68% yield). Mp 193 °C. HRMS (ESI) Calcd for $C_{18}H_{16}O_2N_3F_4S$ ($M + H$)⁺: 414.0894. Found: 414.0897. ¹H NMR (500 MHz, DMSO-*d*₆) δ 8.41 (t, $J = 5.6$ Hz, 1H), 7.76–7.66 (m, 2H), 7.39 (dd, $J = 7.7, 7.7$ Hz, 1H), 6.12 (s, 1H), 4.02 (s, 2H), 3.23 (qd, $J = 5.5, 7.2$ Hz, 2H), 2.30 (s, 3H), 1.09 (t, $J = 7.2$ Hz, 3H). ¹³C NMR (126 MHz, DMSO) δ 162.49, 161.65, 158.39, 157.09 (d, $J_{CF} = 254.0$ Hz), 157.05, 136.58 (d, $J_{CF} = 4.5$ Hz), 128.53, 126.65 (d, $J_{CF} = 14.6$ Hz), 125.82 (q, $J_{CF} = 4.7$ Hz), 124.80 (d, $J_{CF} = 4.3$ Hz), 122.62 (q, $J_{CF} = 272.2$ Hz), 122.53, 116.54 (dq, $J_{CF} = 12.5, 32.4$ Hz), 104.44, 35.12 (d, $J_{CF} = 3.1$ Hz), 33.92, 14.09, 11.41.

7-(2-Chloro-5-cyanobenzyl)-N-ethyl-2-methyl-5-oxo-5H-thiazolo[3,2-a]pyrimidine-3-carboxamide (30). The title compound was prepared from chloride **67** in a manner analogous to **28** (9% yield). LCMS, $m/z = 386.7$ [$M + H$]⁺. ¹H NMR (300 MHz, CDCl₃) δ 7.59 (s, 1H), 7.50 (s, 2H), 6.05 (s, 1H), 5.82 (m, 1H), 4.03 (s, 2H), 3.55–3.51 (m, 2H), 2.44 (s, 3H), 1.28 (t, $J = 7.2$ Hz, 3H).

7-(5-Cyano-2-cyclopropylbenzyl)-N-ethyl-2-methyl-5-oxo-5H-thiazolo[3,2-a]pyrimidine-3-carboxamide (31). The title compound was prepared from chloride **67** in a manner analogous to **28** (14% yield). HRMS (ESI) Calcd for $C_{21}H_{21}N_4O_2S$ ($M + H$)⁺: 393.1380. Found: 393.1390. ¹H NMR (300 MHz, CDCl₃) δ 7.47–7.44 (m, 1H), 7.32–7.19 (m, 2H), 5.94 (s, 1H), 5.83–5.81 (m, 1H), 4.16 (s, 2H), 3.56–3.52 (m, 2H), 2.41 (s, 3H), 1.92–1.82 (m, 1H), 1.28 (t, $J = 7.2$ Hz, 3H), 1.02–0.96 (m, 2H), 0.70–0.65 (m, 2H).

N-Ethyl-7-(1-(2-fluoro-3-(trifluoromethyl)phenyl)ethyl)-2-methyl-5-oxo-5H-thiazolo[3,2-a]pyrimidine-3-carboxamide (32). To a –78 °C solution of ethyl amide **29** (200 mg, 0.48 mmol) in tetrahydrofuran (20 mL) was added *n*-butyllithium (2.5 M in hexanes; 1 mL). After 30 min at –78 °C, iodomethane (235 mg, 1.66 mmol) was added. The resulting solution was stirred for 3 h at room temperature. The reaction was then quenched by water (20 mL), extracted with dichloromethane (3 × 30 mL), washed with brine, dried over sodium sulfate, and concentrated *in vacuo*. The residue was purified by chromatography with dichloromethane/methanol (50:1) to afford the title compound (52.7 mg, 25%) as a white solid. HRMS (ESI) Calcd for $C_{19}H_{18}F_3N_3O_2S$ ($M + H$)⁺: 428.1050. Found: 428.1059. ¹H NMR (300 MHz, CDCl₃) δ 7.60–7.48 (m, 2H), 7.20–7.19 (m, 1H), 6.13 (s, 1H), 5.92 (bs, 1H), 4.38 (q, $J = 7.2$ Hz, 1H), 3.56–3.48 (m, 2H), 2.40 (s, 3H), 1.63 (d, $J = 6.9$ Hz, 3H), 1.28 (t, $J = 7.2$ Hz, 3H).

N-Ethyl-2-methyl-5-oxo-7-((3-(trifluoromethyl)-1H-pyrazol-1-yl)methyl)-5H-thiazolo[3,2-a]pyrimidine-3-carboxamide (33). The title compound was prepared from chloride **67** in a manner analogous to **35** (63% yield). HRMS (ESI) Calcd for $C_{15}H_{15}F_3N_5O_2S$ ($M + H$)⁺: 386.0893. Found: 396.0904. ¹H NMR (400 MHz, DMSO-*d*₆) δ 8.39 (t, $J = 5.6$ Hz, 1H), 8.11 (dd, $J = 2.3, 1.2$ Hz, 1H), 6.80 (d, $J = 2.4$ Hz, 1H), 5.89 (s, 1H), 5.38 (s, 2H), 3.22 (qd, $J = 7.2, 5.5$ Hz, 2H), 2.31 (s, 3H), 1.18–1.05 (m, 3H).

N-Ethyl-2-methyl-7-((5-methyl-3-(trifluoromethyl)-1H-pyrazol-1-yl)methyl)-5-oxo-5H-thiazolo[3,2-a]pyrimidine-3-carboxamide (34). The title compound was prepared from chloride **67** in a manner analogous to **35** (15% yield). HRMS (ESI) Calcd for $C_{16}H_{17}F_3N_5O_2S$ ($M + H$)⁺: 400.1050. Found: 400.1060. ¹H NMR (300 MHz, CDCl₃) δ 6.37 (s, 1H), 5.97 (bs, 1H), 5.93 (s, 1H), 5.18 (s, 2H), 3.56–3.47 (m, 2H), 2.42 (s, 3H), 2.29 (s, 3H), 1.27 (t, $J = 7$ Hz, 3H).

7-(5-Chloro-3-(trifluoromethyl)-1H-pyrazol-1-yl)methyl)-N-ethyl-2-methyl-5-oxo-5H-thiazolo[3,2-a]pyrimidine-3-carboxamide (35). To a solution of chloride **67** (500 mg, 1.75 mmol) in acetonitrile (50 mL) was added 5-chloro-3-(trifluoromethyl)-1H-pyrazole **71** (596 mg, 3.50 mmol), potassium iodide (146 mg, 0.88 mmol), and potassium carbonate (484 mg, 3.50 mmol). The resulting mixture was stirred for 4 h at 80 °C and then cooled to room temperature. The resulting mixture was washed with brine (30 mL), and the solution was extracted with dichloromethane (3 × 50 mL) and concentrated *in vacuo*. The residue was applied onto a prep-TLC with ethyl acetate/petroleum ether (2:1) to afford the title compound (205 mg, 28%) as a white solid. Mp 214 °C. HRMS (ESI) Calcd for $C_{15}H_{14}O_2N_5ClF_3S$ ($M + H$)⁺: 420.0503. Found: 420.0521. ¹H NMR (500 MHz, DMSO-*d*₆) δ 8.44 (t, $J = 5.6$ Hz, 1H), 7.16 (s, 1H), 5.91 (s, 1H), 5.43 (s, 2H), 3.23 (dq, $J = 7.2, 5.6$ Hz, 2H), 2.31 (s, 3H), 1.09 (t, $J = 7.2$ Hz, 3H). ¹³C NMR (126 MHz, DMSO) δ 162.14, 158.53, 158.26, 156.83, 140.91 (q, $J_{CF} = 38.2$ Hz), 129.53, 128.61, 123.18, 120.56 (q, $J_{CF} = 268.7$ Hz), 104.15, 103.17, 52.93, 33.93, 14.08, 11.46.

7-((5-Cyclopropyl-3-(trifluoromethyl)-1H-pyrazol-1-yl)methyl)-N-ethyl-2-methyl-5-oxo-5H-thiazolo[3,2-a]pyrimidine-3-carboxamide (36). The title compound was prepared from chloride **67** in a manner analogous to **35** (32% yield). HRMS (ESI) Calcd for $C_{18}H_{19}F_3N_5O_2S$ ($M + H$)⁺: 426.1206. Found: 426.1217. ¹H NMR (300 MHz, CDCl₃) δ 6.17 (s, 1H), 5.84–5.81 (m, 1H), 5.66 (s, 1H), 5.32 (s, 2H), 3.54–3.49 (m, 2H), 2.43 (s, 3H), 1.68–1.63 (m, 1H), 1.28 (t, $J = 7.2$ Hz, 3H), 1.02–1.00 (m, 2H), 0.75–0.73 (m, 2H).

7-((5-Ethoxy-3-(trifluoromethyl)-1H-pyrazol-1-yl)methyl)-N-ethyl-2-methyl-5-oxo-5H-thiazolo[3,2-a]pyrimidine-3-carboxamide (37). The title compound was prepared from chloride **67** in a manner analogous to **35** (15% yield). HRMS (ESI) Calcd for $C_{17}H_{19}F_3N_5O_3S$ ($M + H$)⁺: 430.1155. Found: 430.1167. ¹H NMR (400 MHz, DMSO-*d*₆) δ 8.41 (t, $J = 5.6$ Hz, 1H), 6.32 (s, 1H), 5.70 (s, 1H), 5.12 (s, 2H),

4.24 (q, $J = 7.0$ Hz, 2H), 3.22 (qd, $J = 7.3$, 5.4 Hz, 2H), 2.32 (s, 3H), 1.31 (t, $J = 7$ Hz, 3H), 1.09 (t, $J = 7$ Hz, 3H).

N-Ethyl-7-((5-isobutoxy-3-(trifluoromethyl)-1H-pyrazol-1-yl)methyl)-2-methyl-5-oxo-5H-thiazolo[3,2-a]pyrimidine-3-carboxamide (38). The title compound was prepared from chloride **67** in a manner analogous to **35** (26% yield). HRMS (ESI) Calcd for $C_{19}H_{23}F_3N_5O_3S$ ($M + H$)⁺: 458.1468. Found: 458.1483. ¹H NMR (400 MHz, DMSO-*d*₆) δ 8.41 (t, $J = 6$ Hz, 1H), 6.31 (s, 1H), 5.76 (s, 1H), 5.13 (s, 2H), 3.96 (d, $J = 7$ Hz, 2H), 3.22 (qd, $J = 8$, 6 Hz, 2H), 2.31 (s, 3H), 1.99 (dq, $J = 13.3$, 7 Hz, 1H), 1.09 (t, $J = 7$ Hz, 3H), 0.91 (d, $J = 7$ Hz, 6H).

7-((Ethyl(4-fluorophenyl)amino)methyl)-3-((1R,2R)-2-(hydroxymethyl)cyclopropyl)-2-methyl-5H-thiazolo[3,2-a]pyrimidin-5-one (39). The title compound was prepared from bromide **48** in a manner analogous to **40** (35% yield). HRMS (ESI) Calcd for $C_{20}H_{23}FN_3O_2S$ ($M + H$)⁺: 388.1490. Found: 388.1500. ¹H NMR (300 MHz, CDCl₃) δ 7.00 (d, $J = 6.9$ Hz, 4H), 6.30 (s, 1H), 4.35 (s, 2H), 4.06 (dd, $J_1 = 6.6$ Hz, $J_2 = 11.4$ Hz, 1H), 3.57 (q, $J = 7.2$ Hz, 2H), 3.13 (t, $J = 10.6$ Hz, 1H), 2.41 (s, 3H), 2.22–2.30 (m, 1H), 1.27–1.31 (m, 4H), 0.99–1.09 (m, 2H).

7-((4-Fluorophenoxy)methyl)-3-((1R,2R)-2-(hydroxymethyl)cyclopropyl)-2-methyl-5H-thiazolo[3,2-a]pyrimidin-5-one (40). To a mixture of bromide **82** (500 mg, 1.35 mmol) in 1,4-dioxane/water (9 mL/3 mL) was added trifluoroborate salt **78** (480 mg, 2.70 mmol), [1,1'-bis(diphenylphosphino)ferrocene]palladium(II) dichloride (200 mg, 0.27 mmol), and sodium carbonate (290 mg, 2.70 mmol). The reaction mixture was irradiated with microwave radiation for 1.5 h at 120 °C. The resulting mixture was concentrated *in vacuo*. The residue was purified by flash chromatography on silica gel eluting with ethyl acetate/petroleum ether (1/2) to afford the racemic product (150 mg, 30%). The racemic product was then separated with SFC with the following conditions (column, Lux μ m Cellulose-3, 2 \times 25 cm; mobile phase, CO₂/EtOH (0.2% DEA) = 65:35; flow rate, 45 g/min; detector, 220 nm) to afford two enantiomers.

Enantiomer 1 (**40**) (peak 1, 68 mg, 14%, white solid). Retention time: 9.93 min. $[\alpha]_D - 96.31$ (c. 0.3, in CH₂Cl₂); HRMS (ESI) Calcd for $C_{18}H_{18}FN_3O_3S$ ($M + H$)⁺: 361.1017. Found: 361.1029. ¹H NMR (500 MHz, DMSO-*d*₆) δ 7.18–7.11 (m, 2H), 7.08–7.02 (m, 2H), 6.21 (s, 1H), 4.94 (s, 2H), 4.59 (t, $J = 5.6$ Hz, 1H), 3.47 (t, $J = 5.8$ Hz, 2H), 2.38 (d, $J = 1.5$ Hz, 3H), 2.06–1.98 (m, 1H), 1.33–1.23 (m, 1H), 0.92–0.80 (m, 2H). ¹³C NMR (126 MHz, DMSO) δ 162.10, 160.29, 159.48, 156.67 (d, $J_{CF} = 236.9$ Hz), 153.90, 133.61, 120.35, 115.96 (d, $J_{CF} = 5.4$ Hz), 115.83 (d, $J_{CF} = 19.3$ Hz), 103.23, 68.51, 63.27, 22.96, 14.77, 12.72, 12.11.

Enantiomer 2 (peak 2, 60 mg, 13%, white solid). Retention time: 11.06 min. LCMS, $m/z = 361.0$ [$M + H$]⁺. ¹H NMR (300 MHz, CDCl₃) δ 7.02–6.89 (m, 4H), 6.47 (s, 1H), 4.91 (s, 2H), 4.08–4.03 (m, 1H), 3.12 (t, $J = 10$, 1 Hz, 1H), 2.40 (s, 3H), 2.30–2.28 (m, 1H), 1.30–1.25 (m, 1H), 1.07–1.01 (m, 2H).

2-Fluoro-3-((3-(2-(hydroxymethyl)cyclopropyl)-2-methyl-5-oxo-5H-thiazolo[3,2-a]pyrimidin-7-yl)methyl)benzonitrile (41). The title compound was prepared from bromide **83** in a manner analogous to **39** (10% yield). LCMS, $m/z = 370.0$ [$M + H$]⁺. ¹H NMR (300 MHz, CDCl₃) δ 7.64–7.57 (m, 2H), 7.29–7.24 (m, 1H), 6.07 (s, 1H), 4.07 (dd, $J = 3.6$, 11.4 Hz, 1H), 3.99 (s, 2H), 3.15 (dd, $J = 9.6$, 11.4 Hz, 1H), 2.41 (s, 3H), 2.32–2.26 (m, 1H), 1.29–1.24 (m, 1H), 1.06–0.99 (m, 2H).

7-(2-Fluoro-3-(trifluoromethyl)benzyl)-3-(2-(hydroxymethyl)cyclopropyl)-2-methyl-5H-thiazolo[3,2-a]pyrimidin-5-one (42). The title compound was prepared from bromide **84** in a manner analogous to **39** (11% yield). HRMS (ESI) Calcd for $C_{19}H_{17}F_4N_2O_2S$ ($M + H$)⁺: 413.0941. Found: 413.0950. ¹H NMR (400 MHz, DMSO-*d*₆) δ 7.76–7.64 (m, 2H), 7.38 (t, $J = 7.8$ Hz, 1H), 6.02 (s, 1H), 4.58–4.51 (m, 1H), 3.96 (s, 2H), 3.50–3.40 (m, 5H), 2.35 (s, 3H), 2.00 (dtd, $J = 8.6$, 5.5, 1.8 Hz, 1H), 1.33–1.20 (m, 1H), 0.93–0.78 (m, 2H).

7-((5-Chloro-3-(trifluoromethyl)-1H-pyrazol-1-yl)methyl)-3-((1R,2R)-2-(hydroxymethyl)cyclopropyl)-2-methyl-5H-thiazolo[3,2-a]pyrimidin-5-one (43). The title compound was prepared from bromide **85** in a manner analogous to **39** (7% yield). HRMS (ESI) Calcd for $C_{16}H_{15}F_3N_4ClO_2S$ ($M + H$)⁺: 419.0551. Found: 419.0565. ¹H NMR (300 MHz, CDCl₃) δ 6.59 (s, 1H), 5.70 (s, 1H), 5.27 (s,

2H), 4.03 (dd, $J = 3.6$, 11.7 Hz, 1H), 3.11 (t, $J = 9.9$ Hz, 2H), 2.39 (s, 3H) 2.30–2.22 (m, 1H) 1.28–1.24 (m, 1H), 1.03–0.97 (m, 2H).

7-((5-Chloro-3-(trifluoromethyl)-1H-pyrazol-1-yl)methyl)-3-((1R,2R)-2-(hydroxymethyl)cyclopropyl)-2-(trifluoromethyl)-5H-thiazolo[3,2-a]pyrimidin-5-one (44). The title compound was prepared from bromide **92** in a manner analogous to **39** (7% yield). HRMS (ESI) Calcd for $C_{16}H_{12}F_6N_4ClO_2S$ ($M + H$)⁺: 473.0268. Found: 473.0284. ¹H NMR (300 MHz, CDCl₃) δ 6.60 (s, 1H), 5.81 (s, 1H), 5.28 (s, 1H), 3.97 (dd, $J = 3.3$, 12 Hz, 1H), 3.23 (dd, $J = 8.4$, 11.4 Hz, 1H), 2.41–2.39 (m, 1H), 1.42–1.33 (m, 2H), 1.10–1.06 (m, 1H).

(1R,2R)-2-(7-((5-Chloro-3-(trifluoromethyl)-1H-pyrazol-1-yl)methyl)-2-methyl-5-oxo-5H-thiazolo[3,2-a]pyrimidin-3-yl)-cyclopropanecarbonitrile (45). The title compound was prepared from bromide **85** in a manner analogous to **46** (38% yield). LCMS, $m/z = 422$ [$M + H$]⁺. ¹H NMR (400 MHz, CD₃OD) δ 6.82 (s, 1H), 5.89 (s, 1H), 5.37 (s, 2H), 2.96–2.91 (m, 1H), 2.45 (s, 3H), 2.00–1.95 (m, 1H) 1.81–1.76 (m, 1H), 1.60–1.55 (m, 1H).

(1R,2R)-2-(7-((5-Chloro-3-(trifluoromethyl)-1H-pyrazol-1-yl)methyl)-5-oxo-2-(trifluoromethyl)-5H-thiazolo[3,2-a]pyrimidin-3-yl)cyclopropanecarbonitrile (46). To a mixture of bromide **92** (350 mg, 0.73 mmol) in 1,4-dioxane/water (15 mL/1.5 mL) was added trifluoroborate salt **81** (350 mg, 2.02 mmol), Pd(dppf)Cl₂ (120 mg, 0.16 mmol), and sodium carbonate (350 mg, 3.30 mmol), and the resulting mixture was stirred overnight at 85 °C. The resulting mixture was filtered and concentrated *in vacuo*. The residue was purified on a silica gel column eluting with ethyl acetate/petroleum ether (1/2). Then the racemic product was separated by Prep-Chiral HPLC with the following conditions (column, CHIRALPAK IC-3, 0.45 \times 5 cm, 3 μ m; mobile phase, Hex/EtOH = 50:50; flow rate, 1.0 mL/min; detector, 254 nm) to afford two enantiomers.

Enantiomer 1 (**46**) (peak 1, 34.5 mg, 10%, white solid). Retention time: 1.461 min; $[\alpha]_D - 586.46$ (c. 0.3, in CH₂Cl₂); mp 137 °C. HRMS (ESI) Calcd for $C_{16}H_9F_6N_5ClOS$ ($M + H$)⁺: 468.0115. Found: 468.0133. ¹H NMR (500 MHz, DMSO-*d*₆) δ 7.16 (s, 1H), 6.05 (s, 1H), 5.43 (s, 2H), 3.08–3.01 (m, 1H), 2.33 (dt, $J = 5.8$, 9.1 Hz, 1H), 1.85 (dt, $J = 5.7$, 8.9 Hz, 1H), 1.49 (dt, $J = 5.9$, 8.8 Hz, 1H). ¹³C NMR (126 MHz, DMSO) δ 161.38, 158.98, 158.87, 141.02 (q, $J_{CF} = 38.2$ Hz), 139.08 (q, $J_{CF} = 4.5$ Hz), 129.65, 121.01 (q, $J_{CF} = 270.6$ Hz), 120.54 (q, $J_{CF} = 268.8$ Hz), 120.44, 113.14 (q, $J_{CF} = 39.2$ Hz), 105.30, 104.15, 52.53, 18.26, 15.00 (q, $J_{CF} = 2.6$ Hz), 5.97.

Enantiomer 2 (peak 2, 34.5 mg, 10%, white solid). Retention time: 2.383 min. HRMS (ESI) Calcd for $C_{16}H_9F_6N_5ClOS$ ($M + H$)⁺: 468.0115. Found: 468.0134. ¹H NMR (400 MHz, CDCl₃) δ 6.60 (s, 1H), 5.81 (s, 1H), 5.27 (s, 2H), 3.11–3.00 (m, 1H), 1.91–1.80 (m, 2H), 1.65–1.62 (m, 1H).

3-Bromo-7-((ethyl(4-fluorophenyl)amino)methyl)-2-methyl-5H-thiazolo[3,2-a]pyrimidin-5-one (48). A mixture of alkyl chloride **47**¹² (30 g, 0.1 mol), *N*-ethyl-4-fluoroaniline (18.5 g, 0.13 mol), potassium carbonate (28.2 g, 0.2 mol), and sodium iodide (7.66 g, 0.05 mol) in acetonitrile was heated overnight at 80 °C. The mixture was then cooled to room temperature, diluted with a saturated aqueous solution of ammonium chloride (300 mL) and extracted with dichloromethane (200 mL \times 3). The combined organic layers were washed with water and brine, dried over sodium sulfate, and concentrated. The residue was triturated with dichloromethane to give the title compound (21 g, 54%) as an off-white solid. LCMS, $m/z = 398.0$ [$M + H$]⁺. ¹H NMR (400 MHz, DMSO-*d*₆) δ 6.98 (t, $J = 8.8$ Hz, 2H), 6.62 (dd, $J = 9.2$, 4.4 Hz, 2H), 5.88 (s, 1H), 4.31 (s, 2H), 3.46 (q, $J = 7.0$ Hz, 2H), 2.32 (s, 3H), 1.13 (t, $J = 7.0$ Hz, 3H).

7-((Ethyl(4-fluorophenyl)amino)methyl)-2-methyl-5-oxo-5H-thiazolo[3,2-a]pyrimidine-3-carbaldehyde (49). To a solution of bromide **48** (200 mg, 0.51 mmol) in tetrahydrofuran (10 mL) was added *n*-butyl lithium (0.3 mL, 2.5 mol/L) at –78 °C. The mixture was then stirred 30 min at the same temperature. Ethyl formate (75.8 mg, 1.02 mmol) was added to the reaction mixture at –78 °C and allowed to warm to room temperature for 1 h. The resulting reaction was quenched by water (20 mL), extracted with dichloromethane (30 mL \times 3), washed with brine, dried over anhydrous sodium sulfate, and concentrated under vacuum. The residue was purified by chromatography with 20% ethyl acetate in petroleum ether to afford the title

compound (60 mg, 35%) as a light yellow solid. LCMS, m/z = 345.1 $[M + H]^+$. 1H NMR (400 MHz, $CDCl_3$) δ 10.76 (s, 1H), 6.95–6.90 (m, 2H), 6.66–6.62 (m, 2H), 6.33 (s, 1H), 4.34 (s, 2H), 3.49 (q, J = 7.2 Hz, 2H), 2.71 (s, 3H), 1.23 (t, J = 7.2 Hz, 3H).

(*E*)-3-(2-Ethoxyvinyl)-7-((ethyl(4-fluorophenyl)amino)methyl)-2-methyl-5H-thiazolo[3,2-*a*]pyrimidin-5-one (**50**). To a solution of bromide **48** (50 mg, 0.13 mmol) in 1,4-dioxane/water (0.6/0.2 mL) was added 2-[(*E*)-2-ethoxyethenyl]-4,4,5,5-tetramethyl-1,3,2-dioxaborolane (40 mg, 0.20 mmol), potassium phosphate (80 mg, 0.38 mmol), and tetrakis(triphenylphosphine)palladium (20 mg, 0.02 mmol). The resulting solution was stirred for 3 h at 90 °C under nitrogen. After cooling to room temperature, the reaction mixture was concentrated *in vacuo*. The residue was purified by chromatography with ethyl acetate/petroleum ether (1/5) to afford the title compound (16.9 mg, 35%) as a light yellow solid. LCMS, m/z = 388.0 $[M + H]^+$. 1H NMR δ (300 MHz, $CDCl_3$) δ 6.93–6.85 (m, 2H), 6.60–6.51 (m, 2H), 6.49 (d, J = 12.9 Hz, 1H), 6.29 (d, J = 12.9 Hz, 1H), 6.10 (s, 1H), 4.27 (s, 2H), 3.96 (q, J = 6.9 Hz, 2H), 3.42–3.53 (q, J = 6.9 Hz, 2H), 2.38 (s, 3H), 1.36 (t, J = 6.9 Hz, 3H), 2.21 (t, J = 6.9 Hz, 3H).

(*E*)-Ethyl 3-(7-((ethyl(4-fluorophenyl)amino)methyl)-2-methyl-5-oxo-5H-thiazolo[3,2-*a*]pyrimidin-3-yl)acrylate (**51**). To a solution of bromide **48** (400 mg, 1.01 mmol), tri(*o*-tolyl)phosphine (60 mg, 0.20 mmol), triethylamine (200 mg, 1.98 mmol), and tris(dibenzylideneacetone)dipalladium(0) (50 mg, 0.05 mmol) in acetonitrile (20 mL) was added ethyl acrylate (200 mg, 2.00 mmol). The reaction mixture was stirred for 3 h at 90 °C and then concentrated *in vacuo*. The residue was purified by chromatography with ethyl acetate/petroleum ether (1/2) to afford the title compound (280 mg, 67%) as a light yellow solid. LCMS, m/z = 416.0 $[M + H]^+$. 1H NMR (400 MHz, $CDCl_3$) δ 8.23 (d, J = 16.4 Hz, 1H), 6.94–6.90 (m, 2H), 6.62–6.59 (m, 2H), 6.20 (s, 1H), 5.98 (d, J = 16.4 Hz, 1H), 4.31–4.27 (m, 4H), 3.50–3.47 (m, 2H), 2.48 (s, 3H), 1.37–1.22 (m, 6H).

4-Cyclobutyl-5-methyl-1,3-thiazol-2-amine (**56**). To a solution of 2-bromo-1-cyclobutylpropan-1-one (3.50 g, 31.3 mmol) in ethanol (30 mL) was added thiourea (1.5 g, 19.71 mmol). The reaction was heated to reflux for 1 h and then concentrated *in vacuo*. The residue was then dissolved in dichloromethane (50 mL), and the solids were filtered off. The resulting solution was concentrated *in vacuo* to afford the title compound (600 mg, 18%) as a yellow solid. LCMS, m/z = 169.0 $[M + H]^+$. 1H NMR (300 MHz, $CDCl_3$) δ 4.92 (brs, 2H), 3.50–3.39 (m, 1H), 2.42–2.17 (m, 4H), 2.16 (s, 3H), 2.04–1.92 (m, 2H).

7-(Chloromethyl)-3-cyclobutyl-2-methyl-5H-thiazolo[3,2-*a*]pyrimidin-5-one (**60**). To a solution of aminothiazole **56** (335 mg, 1.99 mmol) was added polyphosphoric acid (5 mL) and ethyl 4-chloro-3-oxobutanoate (492 mg, 2.99 mmol), and the reaction solution was stirred for 1 h at 110 °C. The pH of the solution was then adjusted to pH 9–10 with an aqueous sodium hydroxide solution (2 M). The reaction mixture was then extracted with dichloromethane (5 \times 100 mL), washed with brine, dried over sodium sulfate and concentrated *in vacuo* to afford the title compound (300 mg, 56%) as a brown solid. The crude product was used in next step without further purification. LCMS, m/z = 269.0 $[M + H]^+$. 1H NMR (300 MHz, $CDCl_3$) δ 6.30 (s, 1H), 4.49–4.40 (m, 1H), 4.36 (s, 2H), 2.41 (s, 3H), 2.39–2.27 (m, 4 H), 2.10–1.94 (m, 1H), 1.89–1.80 (m, 1H).

2-Amino-*N*-ethyl-5-methylthiazole-4-carboxamide (**65**). Into a sealed tube was added methyl 2-amino-5-methyl-1,3-thiazole-4-carboxylate (10.0 g, 58.0 mmol) and ethyl amine in ethanol (80 mL). After stirring overnight at 120 °C in an oil bath, the reaction mixture was concentrated *in vacuo* to afford the title compound (10 g, 84%) as an off-white solid, which was used in the next step without further purification. LCMS, m/z = 186.0 $[M + H]^+$. 1H NMR (400 MHz, CD_3OD) δ 3.36–3.31 (m, 2H), 2.57 (s, 3H), 1.08 (t, J = 7.2 Hz, 3H).

7-(Chloromethyl)-*N*,2-dimethyl-5-oxo-5H-thiazolo[3,2-*a*]pyrimidine-3-carboxamide (**66**). The title compound was prepared in a manner analogous to **67** (60% yield, 4 steps). LCMS, m/z = 272.0 $[M + H]^+$. 1H NMR (400 MHz, $DMSO-d_6$) δ 8.38 (q, J = 4.8 Hz, 1 H); 6.39 (s, 1 H); 4.60 (s, 2 H); 2.74 (d, J = 4.8 Hz, 3 H); 2.30 (s, 3 H).

7-(Chloromethyl)-*N*-ethyl-2-methyl-5-oxo-5H-thiazolo[3,2-*a*]pyrimidine-3-carboxamide (**67**). Into a 2-L three-necked round-bottom flask were placed amine **65** (70 g, 377.87 mmol), ethyl 4-chloro-3-oxobutanoate (281.46 g, 1.71 mol), and PPA (700 g, 4.24 mol). The resulting mixture was stirred at 110 °C for 2 h, cooled to 80 °C, and then quenched by the addition of 200 mL of water. The pH of the solution was adjusted to pH 8 with sodium hydroxide (10%). The resulting solids were then filtered off, and the filtrate was extracted with dichloromethane (5 L \times 5). The combined organic layers were concentrated under vacuum, and the residue was purified on a silica gel column eluting with dichloromethane/methanol (20/1) to give the title compound (52 g, 48%) as a brown solid. LCMS, m/z = 386.0 $[M + H]^+$. 1H NMR (300 MHz, $DMSO-d_6$) δ 8.42 (t, J = 5.5 Hz, 1 H); 6.39 (s, 1 H); 4.59 (s, 2 H); 3.32–3.19 (m, 2 H); 2.33 (s, 3 H); 1.08 (t, J = 7.2 Hz, 3 H).

N,N-Dimethyl-3-(trifluoromethyl)-1H-pyrazole-1-sulfonamide (**69**). Into a 20-L four-necked round-bottom flask purged and maintained with an inert atmosphere of nitrogen were placed 3-(trifluoromethyl)-1H-pyrazole (**68**) (1 kg, 7.35 mol), acetonitrile (10 L), and 1,4-diazabicyclo[2.2.2]octane (990 g, 8.83 mol) followed by the dropwise addition of *N,N*-dimethylsulfamoyl chloride (1.16 kg, 8.05 mol) with stirring at 0 °C. The resulting solution was stirred at room temperature for 3 h, concentrated under vacuum, diluted with 10 L of H_2O , and extracted with ethyl acetate (3 \times 5L). The combined organic layers were washed with 2 \times 5 L of brine, dried over anhydrous sodium sulfate and concentrated under vacuum. The residue was applied onto a silica gel column eluting with dichloromethane to afford the title compound (1.7 kg, 95%) as a colorless oil. LCMS, m/z = 244 $[M + H]^+$. 1H NMR (300 MHz, $CDCl_3$) δ 8.02 (d, J = 2.7 Hz, 1H), 6.40 (d, J = 2.7 Hz, 1H), 3.00 (s, 6H).

5-Chloro-*N,N*-dimethyl-3-(trifluoromethyl)-1H-pyrazole-1-sulfonamide (**70**). Into a 5 L four-necked round-bottom flask purged and maintained with an inert atmosphere of nitrogen were placed tetrahydrofuran (3 L) and pyrazole **69** (240 g, 987 mmol), followed by the dropwise addition of 2.5 M *n*-BuLi (480 mL) with stirring at –70° for 1 h. To this mixture was added hexachloroethane (323 g, 1.36 mol) at –70 °C for an additional 2 h. The reaction mixture was then quenched with 2 L of saturated aqueous NH_4Cl and then extracted with 2 \times 2 L of dichloromethane. The combined organic layers were washed with 1 L of brine, dried over anhydrous sodium sulfate and concentrated under vacuum to afford the title compound (240 g, 88%) as a brown oil, which was carried forward to the next step without further purification. LCMS, m/z = 278 $[M + H]^+$. 1H NMR (300 MHz, $CDCl_3$) δ 6.58 (s, 1H), 3.15 (s, 6H).

5-Chloro-3-(trifluoromethyl)-1H-pyrazole (**71**). Into a 10 L four-necked round-bottom flask was placed crude pyrazole **70** (2.2 kg, 7.92 mol) in dichloromethane (2 L) followed by the dropwise addition of trifluoroacetic acid (1.5 L) with stirring at 0 °C. The resulting solution was stirred at room temperature for 5 h, concentrated under vacuum, and diluted with 6 L of H_2O . The pH of the solution was adjusted to pH 8–9 with sodium bicarbonate. The resulting solution was extracted with 3 \times 4 L of ethyl acetate. The combined organic layers were dried over anhydrous sodium sulfate and concentrated under vacuum. The crude product was purified by distillation under reduced pressure (15 mmHg), and the fraction was collected at 52–65 °C. The crude product was recrystallized from DCM/hexane in the ratio of 1:50 to afford the title compound (520 g, 38%) as a white solid. LCMS, m/z = 171 $[M + H]^+$. 1H NMR (300 MHz, $CDCl_3$) δ 8.22–8.40 (brs, 1H), 6.56 (s, 1H).

1-Cyclopropyl-4,4,4-trifluorobutane-1,3-dione (**74**). Into a 3000 mL four-necked round-bottom flask purged and maintained with an inert atmosphere of nitrogen were placed 1-cyclopropylethan-1-one (100 g, 1.19 mol), ethanol (2000 mL), and ethyl trifluoroacetate (169 g, 1.19 mol), followed by the addition of Na (32.8 g, 1.43 mol) in several batches at 0–20 °C. The resulting solution was stirred at room temperature for 48 h, concentrated under vacuum, and then diluted with 1000 mL of H_2O . The pH value of the solution was adjusted to 4–5 with hydrogen chloride (6 mol/L), and the resulting solution was extracted with 4 \times 1000 mL of dichloromethane. The combined organic layers were dried over anhydrous sodium sulfate and

concentrated under vacuum to afford 70 g (33%) of the title compound as a yellow oil.

3-Cyclopropyl-5-(trifluoromethyl)-1H-pyrazole (75). Into a 1000 mL round-bottom flask purged and maintained with an inert atmosphere of nitrogen were placed 1,3-diketone **74** (51 g, 283.14 mmol), methanol (500 mL), $\text{N}_2\text{H}_4\cdot\text{H}_2\text{O}$ (98%) (15.3 g, 283 mmol), and acetic acid (70 mL). The resulting solution was heated to reflux overnight, concentrated under vacuum, and then diluted with 500 mL of H_2O . The pH value of the solution was adjusted to 9 with sodium carbonate (solid), and the resulting solution was extracted with 3×200 mL of ethyl acetate. The combined organic layers were washed with 1×200 mL of H_2O and 2×200 mL of brine, dried over anhydrous sodium sulfate, and concentrated under vacuum to afford 44 g (88%) of the title compound as a light yellow solid. LCMS, $m/z = 177$ $[\text{M} + \text{H}]^+$. ^1H NMR (300 MHz, CDCl_3) δ 0.75–0.79 (m, 2H), 1.01–1.08 (m, 2H), 1.87–1.96 (m, 1H), 6.19 (s, 1H), 9.59 (s, 1H).

tert-Butyldimethyl((trans-2-(4,4,5,5-tetramethyl-1,3,2-dioxaborolan-2-yl)cyclopropyl)methoxy)silane (77). Diethylzinc (1.0 M in hexane) (200 mL, 200 mmol) was added to freshly distilled dichloromethane (200 mL) under nitrogen. A solution of trifluoroacetic acid (15.4 mL, 200 mmol) in dichloromethane (100 mL) was then added dropwise at 0°C . Upon stirring for 30 min, a solution of diiodomethane (16.1 mL, 200 mmol) in dichloromethane (100 mL) was added at 0°C . After an additional 30 min of stirring, a solution of (*E*)-tert-butyldimethyl(3-(4,4,5,5-tetramethyl-1,3,2-dioxaborolan-2-yl)-allyloxy)silane (**76**; 30.0 g, 100 mmol) in dichloromethane (100 mL) was added at 0°C . The resulting solution was stirred 2 h at room temperature and was then quenched with water. The reaction was extracted with dichloromethane ($1000\text{ mL} \times 2$) and washed with brine, and the organic layer was then dried over anhydrous sodium sulfate and concentrated to afford the title compound (30 g, 96%) as a colorless oil. ^1H NMR (300 MHz, CDCl_3) δ 3.58–3.53 (m, 1H), 3.44–3.38 (m, 1H), 1.17 (s, 12H), 0.87 (s, 9H), 0.66–0.63 (m, 1H), 0.54–0.49 (m, 1H), 0.06 (s, 6H), –0.35 to –0.25 (m, 2H).

Potassium trans-2-(Hydroxymethyl)cyclopropyltrifluoroborate (78). To a solution of cyclopropane **77** (30.0 g, 100 mmol) in methanol (300 mL) was added a solution of potassium bifluoride (32.0 g, 400 mmol) in water (100 mL) dropwise at 0°C . After stirring 1.5 h at room temperature, the reaction mixture was concentrated under reduced pressure. The resulting solid was suspended in acetone (1 L) and was refluxed 20 min. The heterogeneous mixture was then filtered to remove potassium difluoride, and the filtrate was concentrated. The extraction was repeated for the filtered solid. The combined filtrates were concentrated and dissolved in minimal acetone followed by the slow addition of ethyl ether until the solution become cloudy. The mixture was filtered, and the solid was collected to provide the title compound (7.00 g, 40%) as a white solid. ^1H NMR (300 MHz, CDCl_3) δ 4.01–3.97 (m, 1H), 3.44–3.37 (m, 1H), 2.83–2.75 (m, 1H), 0.58–0.48 (m, 1H), 0.01–0.03 (m, 1H), –0.21 to –0.25 (m, 1H), –0.94 to –0.97 (m, 1H).

2-(4,4,5,5-Tetramethyl-1,3,2-dioxaborolan-2-yl)-cyclopropanecarbonitrile (80). To a solution of bis(pinacolato)diboron (360 g, 1.42 mol) and cyclopropanecarbonitrile (123.85 g, 1.85 mol) in anhydrous THF (1.8 L) was added 2,9-dimethyl-1,10-phenanthroline (11.8 g, 56.8 mmol, J&K) followed by $[\text{Ir}(\text{COD})\text{-OMe}]_2$ (37.7 g, 56.8 mmol, TCI) at 25°C under N_2 . Then the mixture was heated to 90°C and stirred for 18 h. TLC (petroleum ether/ethyl acetate = 10/1, $R_f = 0.65$, KMnO_4) showed that the reaction was complete. Two reactions were combined for workup. The reaction mixture was concentrated in vacuum to give a crude product. The crude product was purified by flash chromatography eluted with petroleum ether/ethyl acetate (from 200/1 to 20/1) twice (the process was monitored by TLC and ^1H NMR) to give crude compound **80** (205 g, yield 37%) as a yellow semisolid, which was used directly in the next step without further purification.

Potassium 2-Cyanocyclopropyltrifluoroborate (81). To a suspension of crude compound **80** (205 g, 1.06 mol) from the previous reaction in MeOH (2.5 L) and H_2O (1.6 L) was added KHF_2 (413.9 g, 5.3 mol) at 25°C . The mixture was then stirred at 25°C for 12 h. The resulting mixture was concentrated in vacuum to remove all of the

solvent, and then the residue was washed with acetone ($1\text{ L} \times 5$). The filtrate was concentrated *in vacuo* and then dissolved in water (800 mL) and washed with ethyl acetate ($1\text{ L} \times 3$) and DCM ($1\text{ L} \times 3$). The aqueous layer was dried by lyophilization to give crude trifluoroborate salt **81** (130 g, yield: 71%) as a white solid, which was used in the next step without further purification. ^1H NMR (300 MHz, $\text{DMSO}-d_6$) δ 0.88–0.82 (m, 1H), 0.76–0.72 (m, 1H), 0.59–0.51 (m, 1H), 0.05–0.11 (m, 1H).

3-Bromo-7-((4-fluorophenoxy)methyl)-2-methyl-5H-thiazolo[3,2-*a*]pyrimidin-5-one (82). The title compound was prepared from chloride **47** in a manner analogous to **48** (80% yield). LCMS, $m/z = 369.1$, 371.1 $[\text{M} + \text{H}]^+$. ^1H NMR (300 MHz, CDCl_3) δ 7.01–6.95 (m, 2H), 6.92–6.86 (m, 2H), 6.44 (s, 1H), 4.88 (s, 2H), 2.36 (s, 3H).

3-((3-Bromo-2-methyl-5-oxo-5H-thiazolo[3,2-*a*]pyrimidin-7-yl)-methyl)-2-fluorobenzonitrile (83). The title compound was prepared from chloride **47** in a manner analogous to **28** (23% yield). LCMS, $m/z = 378.0$ $[\text{M} + \text{H}]^+$. ^1H NMR (400 MHz, $\text{DMSO}-d_6$) δ 7.87–7.81 (m, 1H), 7.75 (t, $J = 7.6$ Hz), 7.38 (t, $J = 7.8$ Hz, 1H), 6.10 (s, 1H), 3.97 (s, 2H), 2.30 (s, 3H).

3-Bromo-7-(2-fluoro-3-(trifluoromethyl)benzyl)-2-methyl-5H-thiazolo[3,2-*a*]pyrimidin-5-one (84). The title compound was prepared from chloride **47** in a manner analogous to **29** (28% yield). LCMS, $m/z = 421.0$ $[\text{M} + \text{H}]^+$. ^1H NMR (300 MHz, CDCl_3) δ 7.53 (t, $J = 7.4$ Hz, 1H), 7.48 (t, $J = 7.2$ Hz, 1H), 7.21 (t, $J = 7.8$ Hz, 1H), 6.02 (s, 1H), 3.94 (s, 2H), 2.34 (s, 3H).

3-Bromo-7-((5-chloro-3-(trifluoromethyl)-1H-pyrazol-1-yl)-methyl)-2-methyl-5H-thiazolo[3,2-*a*]pyrimidin-5-one (85). The title compound was prepared from chloride **47** in a manner analogous to **35** (62% yield). LCMS, $m/z = 429.0$ $[\text{M} + \text{H}]^+$. ^1H NMR (400 MHz, CDCl_3) δ 6.58 (s, 1H), 5.71 (s, 1H), 5.25 (s, 2H), 2.36 (s, 3H).

5-Bromo-2-chlorothiazole (87). To a solution of 5-bromo-1,3-thiazol-2-amine **86** (100 g, 0.56 mol) in CH_3CN (1000 mL) was added CuCl (82 g, 0.83 mol). *t*-BuONO (110 g, 1.08 mol) was then added dropwise with stirring at room temperature. The reaction mixture was stirred for 1 h at room temperature and then stirred for an additional 1 h at 70°C . The reaction was then quenched by the addition of water. The reaction mixture was extracted with diethyl ether, washed with brine, dried over anhydrous sodium sulfate, and concentrated *in vacuo*. The residue was purified by chromatography with diethyl ether/petroleum ether (1:10) to afford the title compound (40 g, 37%) as a light yellow solid. LCMS, $m/z = 199.8$ $[\text{M} + \text{H}]^+$. ^1H NMR (400 MHz, CDCl_3) δ 7.51 (s, 1H).

4-Bromo-2-chloro-5-iodothiazole (88). To a solution of thiazole **87** (40 g, 0.20 mol) in tetrahydrofuran (600 mL) was added LDA (120 mL, 0.24 mol, 2 mol/L in THF) dropwise with stirring at -78°C . The resulting mixture was stirred for 30 min at -78°C . Then a solution of I_2 (77 g, 0.31 mol) in tetrahydrofuran (200 mL) was added dropwise with stirring at -78°C . The resulting solution was slowly warmed to room temperature and then stirred an additional 2 h at which point the reaction was quenched by the addition of water. The reaction mixture was extracted with dichloromethane, washed with brine, dried over anhydrous sodium sulfate, and concentrated *in vacuo*. The residue was purified by chromatography with ethyl acetate/petroleum ether (1:50) to afford the title compound (45 g, 70%) as an off-white solid. LCMS, $m/z = 325.7$ $[\text{M} + \text{H}]^+$.

4-Bromo-2-chloro-5-(trifluoromethyl)thiazole (89). To a mixture of thiazole **88** (45 g, 0.14 mol) and CuI (40 g, 0.21 mol) in N,N -dimethylformamide (500 mL) was added methyl 2,2-difluoro-2-(fluorosulfonyl)acetate (41 g, 0.21 mol). The resulting mixture was stirred overnight at 80°C under nitrogen atmosphere. After filtration, the filtrate was extracted with diethyl ether and washed with brine, dried over anhydrous sodium sulfate, and concentrated *in vacuo*. The residue was purified by chromatography with diethyl ether/petroleum ether (1:10) to afford the title compound (40 g) as a light yellow oil, which was used in the next step without further purification. GCMS, $m/z = 265$, 267 $[\text{M} + \text{H}]^+$.

4-Bromo-5-(trifluoromethyl)thiazol-2-amine (90). To a solution of thiazole **89** (40 g, 0.15 mol) in 1,4-dioxane (250 mL) was added $\text{NH}_3/\text{H}_2\text{O}$ (250 mL, 30% in water). The resulting mixture was stirred overnight at 50°C . The reaction mixture was then extracted with ethyl

acetate, washed with brine, dried over anhydrous sodium sulfate, and concentrated *in vacuo*. The residue was purified on a silica gel column eluted with ethyl acetate/petroleum ether (1:5) to afford the title compound (10 g, 27%) as a light yellow solid. LCMS, m/z = 248.8 $[M + H]^+$. 1H NMR (300 MHz, $CDCl_3$) δ 5.61 (brs, 2H).

3-Bromo-7-(chloromethyl)-2-(trifluoromethyl)-5H-thiazolo[3,2-*a*]pyrimidin-5-one (91). To a mixture of aminothiazole **90** (10 g, 0.040 mol) and ethyl 4-chloro-3-oxobutanoate (33 g, 0.20 mol) was added PPA (100 g). The resulting mixture was stirred overnight at 130 °C in an oil bath. The reaction was then quenched with water at 80 °C. After the mixture cooled to room temperature, the pH of the mixture was adjusted to pH 7 with aqueous NaOH (1 N). The reaction mixture was then extracted with dichloromethane, washed with brine, dried over anhydrous sodium sulfate, and concentrated *in vacuo*. The residue was purified on a silica gel column eluted with ethyl acetate/petroleum ether (1:10) to afford the title compound (8 g, 57%) as a light yellow solid. LCMS, m/z = 348.9 $[M + H]^+$. 1H NMR (400 MHz, $CDCl_3$) δ 6.47 (s, 1H), 4.39 (s, 2H).

3-Bromo-7-((5-chloro-3-(trifluoromethyl)-1H-pyrazol-1-yl)-methyl)-2-(trifluoromethyl)-5H-thiazolo[3,2-*a*]pyrimidin-5-one (92). To a mixture of chloride **91** (1 g, 2.88 mmol) and sodium carbonate (610 mg, 5.75 mmol) in acetonitrile (10 mL) was added pyrazole **71** (590 mg, 3.45 mmol). The resulting mixture was stirred overnight at 80 °C. After filtration and concentration, the residue was purified on a silica gel column eluting with ethyl acetate/petroleum ether (1/20) to afford the title compound (450 mg, 33%) as a light yellow solid. LCMS, m/z = 480.9 $[M + H]^+$. 1H NMR (400 MHz, $CDCl_3$) δ 6.60 (s, 1H), 5.60 (s, 1H), 5.79 (s, 1H), 5.26 (s, 2H).

Pharmaceutical and Biological Assay Protocols. Cell Lines. Doxycycline-inducible (Dox) cell lines that express either GluN1/GluN2A or GluN1/GluN2B were generated in both CHO and HEK293 parental cell lines, and Dox-inducible cell lines that express either GluN1/GluN2C or GluN1/GluN2D were obtained from Chantest Inc. The cDNA for Dox-inducible cell lines that express either the flip or flop isoform of the human GluA2 AMPA receptor included a glutamine at position 607 to impart Ca^{2+} permeability (which is absent when there is an arginine at this position as normally results from highly efficient RNA editing of the glutamine codon at this position in genomic DNA) in order to enable Ca^{2+} influx assays.

Calcium Influx Dose–Response Assays. Compounds were tested for their ability to potentiate either NMDA receptors or AMPA receptors using 384-well calcium influx assays using either an FDSS 7000 or a FLIPR Tetra instrument.

NMDA Receptor Assays. Inducible cell lines expressing either GluN2A-, GluN2B-, GluN2C-, or GluN2D-containing NMDARs were harvested with Detachin (Gentis) and seeded into 384-well poly(D-lysine) coated plates. Expression was induced with the addition of 2 μ g/mL doxycycline overnight in the presence of 500 μ M ketamine to protect the cells. Following the overnight induction, cells were washed and loaded with BD calcium indicator dye in assay buffer for 50 min. For each assay day, the EC_{30} for glutamate was determined using a glutamate dose–response. Compound plates with test compounds were added by the FDSS at 2 \times concentration in 2 \times EC_{30} glutamate, and the resulting fluorescence response was recorded over a 5 min test interval. Saturating glycine was present throughout. Dose–responses were determined using a 10 point 1:2 serial dilution pattern.

AMPA Receptor Assays. Inducible cell lines expressing either the flip or flop splice variants of GluA2 were harvested with Detachin (Gentis) and seeded into 384-well poly(D-lysine) coated plates. Expression was induced with the addition of 5 μ g/mL doxycycline overnight. Following overnight induction, cells were washed and loaded with BD calcium indicator dye in assay buffer for 50 min. Compound plates with test compounds were added by the FDSS at 2 \times concentration in 2 \times 100 μ M glutamate, and the resulting fluorescence response was recorded over a 5 min test interval. Dose–responses were determined using a 10 point 1:2,1:3 serial dilution pattern. The maximum signal in the GluA2 assays (100%) was defined as the AUC achieved using the clinical AMPA receptor PAM, LY450108,²⁸ as a positive control.

Automated Electrophysiology: Measuring Deactivation τ and Fold Deactivation. NMDA receptor currents were recorded on the IonFlux HT (Fluxion Biosciences) automated electrophysiology platform. CHO cells expressing GluN1/GluN2A were harvested, and a suspension of dispersed single cells was applied to the recording plate in high Mg^{2+} buffer to aid seal formation. Once the whole-cell configuration was obtained, recording was performed in zero Mg^{2+} buffer. Cells were first treated with PAMs at 100 μ M (or DMSO vehicle) and 100 μ M glycine for several minutes. PAMs and saturating glycine were continuously applied thereafter. The solution was then rapidly switched to one supplemented with 100 μ M glutamate to activate currents. The solution was then switched back to one without glutamate to measure deactivation. The deactivation time constant, τ , was measured from monoexponential fits to the decay of currents following removal of glutamate. Fold deactivation was calculated by normalizing the PAM τ to the τ measured from wells treated with vehicle.

Whole-Cell Voltage Clamp Electrophysiology with Rapid Solution Exchange. Whole-cell patch clamp recordings from CHO cell lines were obtained using a Molecular Devices Axopatch 200B patch clamp amplifier. The recording pipet intracellular solution contained (in mM): 120 CsF, 10 NaCl, 2 $MgCl_2$, 10 HEPES, adjusted to pH 7.2 with CsOH. The extracellular recording solution contained (in mM): 155 NaCl, 3 KCl, 1.5 $CaCl_2$, 10 HEPES, adjusted to pH 7.4 with NaOH. Currents were recorded at 1 kHz sampling frequency and filtered at 0.2 kHz. Series resistance compensation was applied at 60–80%. In general, the holding voltage was set to –50 mV for the recording of inward GluN2A currents.

Fast perfusion was achieved using the Dynaflo Resolve perfusion system (Celletricon) for rapid solution exchange. This system consists of a quartz glass perfusion chip with a linear array of 16 continuously flowing perfusion channels that are moved past the patched cell with a solution exchange time of approximately 10–30 ms. Recordings were measured in the presence of 50 μ M glycine; 100 μ M glutamate and individual PAMs were applied as depicted in Figures 2 and 5.

■ ASSOCIATED CONTENT

§ Supporting Information

The Supporting Information is available free of charge on the ACS Publications website at DOI: 10.1021/acs.jmedchem.5b02010.

NMR data for key compounds (28, 29, 35, 40, and 46), X-ray crystal structure report, and crystallography statistics (PDF)

Machine-readable compound representations (SMILES) (CSV)

Accession Codes

Coordinates have been deposited in the PDB with the accession codes 5H8H for **2**, 5I2K for **19**, 5I2N for **29**, and 5I2J for **46**. Authors will release the atomic coordinates and experimental data upon article publication.

■ AUTHOR INFORMATION

Corresponding Author

*Tel: 650-467-1305. Fax: 650-742-4943. E-mail: volgraf.matthew@gene.com.

Notes

The authors declare no competing financial interest.

■ ACKNOWLEDGMENTS

We thank the Genentech Analytical, Purification, DMPK, *In vivo* Studies Group, and Safety Assessment colleagues for their contributions. Special thanks to Antonio DePasquale (UC

Berkeley, X-ray Crystallographic Facility) for help determining the absolute stereochemistry of **46**.

■ ABBREVIATIONS

NMDA, *N*-methyl-D-aspartate; NMDAR, *N*-methyl-D-aspartate receptor; PAM, positive allosteric modulator; mGluR, metabotropic glutamate receptor; iGluR, ionotropic glutamate receptor; AMPA, α -amino-3-hydroxy-5-methyl-4-isoxazolepropionic acid; AMPAR, α -amino-3-hydroxy-5-methyl-4-isoxazolepropionic acid receptor; CNS, central nervous system; P-gp, P-glycoprotein; MDCK-MDR1, Madin-Darby canine kidney cells-multidrug resistance protein 1; ER, efflux ratio; PPB, plasma protein binding; BPB, brain protein binding; AUC, area under the curve; MCT, methylcellulose/tween; LBD, ligand binding domain; SAM, silent allosteric modulator; TPSA, topographical polar surface area; BBB, blood-brain barrier; CHO, Chinese hamster ovary; RHS, right-hand side; SAM, silent allosteric modulator; dpfp, 1,1'-bis(diphenylphosphino)-ferrocene; SFC, supercritical fluid chromatography; DCM, dichloromethane; PPA, polyphosphoric acid; HEPES, 4-(2-hydroxyethyl)-1-piperazineethanesulfonic acid; CIQ, (3-chlorophenyl)[3,4-dihydro-6,7-dimethoxy-1-[(4-methoxyphenoxy)methyl]-2(1*H*)-isoquinoliny]-methanone; LDA, lithium diisopropylamide

■ REFERENCES

- (1) Traynelis, S. F.; Wollmuth, L. P.; McBain, C. J.; Menniti, F. S.; Vance, K. M.; Ogden, K. K.; Hansen, K. B.; Yuan, H.; Myers, S. J.; Dingledine, R. Glutamate receptor ion channels: structure, regulation, and function. *Pharmacol. Rev.* **2010**, *62*, 405–496.
- (2) Paoletti, P.; Bellone, C.; Zhou, Q. NMDA receptor subunit diversity: impact on receptor properties, synaptic plasticity and disease. *Nat. Rev. Neurosci.* **2013**, *14*, 383–400.
- (3) Möbius, H. J. Memantine: update on the current evidence. *Int. J. Geriatr. Psychiatry* **2003**, *18*, S47–S54.
- (4) Reynolds, I. J.; Miller, R. J. Ifenprodil is a novel type of *N*-methyl-D-aspartate receptor antagonist: interaction with polyamines. *Mol. Pharmacol.* **1989**, *36*, 758–765.
- (5) Anis, N. A.; Berry, S. C.; Burton, N. R.; Lodge, D. The dissociative anaesthetics, ketamine and phencyclidine, selectively reduce excitation of central mammalian neurons by *N*-methyl-aspartate. *Br. J. Pharmacol.* **1983**, *79*, S65–S75.
- (6) Carlén, M.; Meletis, K.; Siegle, J. H.; Cardin, J. A.; Futai, K.; Vierling-Claassen, D.; Rühlmann, C.; Jones, S. R.; Deisseroth, K.; Sheng, M.; Moore, C. I.; Tsai, L.-H. A critical role for NMDA receptors in parvalbumin interneurons for gamma rhythm induction and behavior. *Mol. Psychiatry* **2012**, *17*, 537–548.
- (7) Grützner, C.; Wibrall, M.; Sun, L.; Rivolta, D.; Singer, W.; Maurer, K.; Uhlhaas, P. J. Deficits in high- (>60 Hz) gamma-band oscillations during visual processing in schizophrenia. *Front. Hum. Neurosci.* **2013**, *7*, 88.
- (8) Ceccon, M.; Rumbaugh, G.; Vicini, S. Distinct effect of pregnenolone sulfate on NMDA receptor subtypes. *Neuropharmacology* **2001**, *40*, 491–500.
- (9) Paul, S. P.; Doherty, J. J.; Robichaud, A. J.; Belfort, G. M.; Chow, B. Y.; Hammond, R. S.; Crawford, D. C.; Linsenbardt, A. J.; Shu, H.-J.; Izumi, Y.; Mennerick, S. J.; Zorumski, C. F. The major brain cholesterol metabolite 24(S)-hydroxycholesterol is a potent allosteric modulator of *N*-Methyl-D-Aspartate Receptors. *J. Neurosci.* **2013**, *33*, 17290–17300.
- (10) Mullasseril, P.; Hansen, K. B.; Vance, K. M.; Ogden, K. K.; Yuan, H.; Kurtkaya, N. L.; Santangelo, R.; Orr, A. G.; Le, P.; Vellano, K. M.; Liotta, D. C.; Traynelis, S. F. A subunit-selective potentiator of NR2C- and NR2D-containing NMDA receptors. *Nat. Commun.* **2010**, *1*, 90.
- (11) Santangelo, R. M.; Ogden, K. K.; Strong, K. L.; Khatri, A.; Chepiga, K. M.; Jensen, H. S.; Traynelis, S. F.; Liotta, D. C. Synthesis and structure activity relationship of tetrahydroisoquinoline-based potentiators of GluN2C and GluN2D containing *N*-methyl-D-aspartate receptors. *J. Med. Chem.* **2013**, *56*, S351–S381.
- (12) Khatri, A.; Burger, P. B.; Swanger, S. A.; Hansen, K. B.; Zimmerman, S.; Karakas, E.; Liotta, D. C.; Furukawa, H.; Snyder, J. P.; Traynelis, S. F. Structural determinants and mechanism of action of a GluN2C-selective NMDA receptor positive allosteric modulator. *Mol. Pharmacol.* **2014**, *86*, S48–S60.
- (13) Sheng, M.; Cummings, J.; Roldan, L. A.; Jan, Y. N.; Jan, L. Y. Changing subunit composition of heteromeric NMDA receptors during development of rat cortex. *Nature* **1994**, *368*, 144–147.
- (14) Ronicke, R.; Mikhaylova, M.; Ronicke, S.; Meinhardt, J.; Schroder, U. H.; Fandrich, M.; Reiser, G.; Kreutz, M. R.; Reymann, K. G. Early neuronal dysfunction by amyloid beta oligomers depends on activation of NR2B-containing NMDA receptors. *Neurobiol. Aging* **2011**, *32*, 2219–2228.
- (15) Ferreira, I. L.; Bajouco, L. M.; Mota, S. I.; Auberson, Y. P.; Oliveira, C. R.; Rego, A. C. Amyloid beta peptide 1–42 disturbs intracellular calcium homeostasis through activation of GluN2B-containing *N*-methyl-d-aspartate receptors in cortical cultures. *Cell Calcium* **2012**, *51*, 95–106.
- (16) Paoletti, P.; Bellone, C.; Zhou, Q. NMDA receptor subunit diversity: impact on receptor properties, synaptic plasticity and disease. *Nat. Rev. Neurosci.* **2013**, *14*, 383–400.
- (17) Hackos, D. H.; Lupardus, P. J.; Grand, T.; Chen, Y.; Wang, T.-M.; Reynen, P.; Gustafson, A.; Wallweber, H. J. A.; Volgraf, M.; Sellers, B. D.; Schwarz, J.; Paoletti, P.; Sheng, M.; Zhou, Q.; Hanson, J. E. Positive allosteric modulators of GluN2A-containing NMDARs with distinct modes of action and impacts on circuit function. *Neuron* **2016**, *89*, 983.
- (18) Wager, T. T.; Hou, X.; Verhoest, P. R.; Villalobos, A. Moving beyond rules: the development of a central nervous system multiparameter optimization (CNS MPO) approach to enable alignment of druglike properties. *ACS Chem. Neurosci.* **2010**, *1*, 435–449.
- (19) Furukawa, H.; Singh, S. K.; Mancusso, R.; Gouaux, E. Subunit arrangement and function in NMDA receptors. *Nature* **2005**, *438*, 185–192.
- (20) Jin, R.; Clark, R.; Weeks, A. M.; Dudman, J. T.; Gouaux, E.; Partin, K. M. Mechanism of positive allosteric modulators acting on AMPA receptors. *J. Neurosci.* **2005**, *25*, 9027.
- (21) Ahmed, A. H.; Ptak, C. P.; Oswald, R. E. Molecular mechanism of flop selectivity and subsite recognition for an AMPA receptor allosteric modulator: structures of GluA2 and GluA3 in complexes with PEPA. *Biochemistry* **2010**, *49*, 2843–2850.
- (22) Shaffer, C. L.; Hurst, R. S.; Scialis, R. J.; Osgood, S. M.; Bryce, D. K.; Hoffmann, W. E.; Lazzaro, J. T.; Hanks, A. N.; Lotarski, S.; Weber, M. L.; Liu, J.-H.; Menniti, F. S.; Schmidt, C. J.; Hajós, M. Positive allosteric modulation of AMPA Receptors from efficacy to toxicity: the interspecies exposure-response continuum of the novel potentiator PF-4778574. *J. Pharmacol. Exp. Ther.* **2013**, *347*, 212–214.
- (23) Harder, M.; Kuhn, B.; Diederich, F. Efficient stacking on protein amide fragments. *ChemMedChem* **2013**, *8*, 397–404.
- (24) Ward, S. E.; Harries, M.; Aldegheri, L.; Austin, N. E.; Ballantine, S.; Ballini, E.; Bradley, D. M.; Bax, B. D.; Clarke, B. P.; Harris, A. J.; Harrison, S. A.; Melarange, R. A.; Mookherjee, C.; Mosley, J.; Dal Negro, G.; Oliosi, B.; Smith, K. J.; Thewlis, K. M.; Wollard, P. M.; Yusaf, S. P. Integration of lead optimization with crystallography for a membrane-bound ion channel target: discovery of a new class of AMPA receptor positive allosteric modulators. *J. Med. Chem.* **2011**, *54*, 78–94.
- (25) Lorenz, J. C.; Long, J.; Yang, Z.; Xue, S.; Xie, X.; Shi, Y. A novel class of tunable zinc reagents (RXZnCH₂Y) for efficient cyclopropanation of olefins. *J. Org. Chem.* **2004**, *69*, 327–334.
- (26) Liskey, C. W.; Hartwig, J. F. Iridium-catalyzed C–H borylation of cyclopropanes. *J. Am. Chem. Soc.* **2013**, *135*, 3375–3378.

(27) Schnürch, M.; Spina, M.; Farook Khan, A.; Mihovilovic, M. D.; Stanetty, P. Halogen dance reactions – a review. *Chem. Soc. Rev.* **2007**, 36, 1046–1057.

(28) Jhee, S. S.; Chappell, A. S.; Zarotsky, V.; Moran, S. V.; Rosenthal, M.; Kim, E.; Chalon, S.; Toubanc, N.; Brandt, J.; Coutant, D. E.; Ereshefsky, L. Multiple-dose plasma pharmacokinetic and safety study of LY450108 and LY451395 (AMPA receptor potentiators) and their concentration in cerebrospinal fluid in healthy human subjects. *J. Clin. Pharmacol.* **2006**, 46, 424–432.